A FOURIER TRANSFORM TO DETECT PINE SEEDLINGS IN A DIGITAL IMAGE

By

DOUGLAS ROBERT DEVOE

Bachelor of Science
Oklahoma State University
Stillwater, Oklahoma
1980

Master of Science
Oklahoma State University
Stillwater, Oklahoma
1982

Submitted to the Faculty of the
Graduate College of the
Oklahoma State University
in partial fulfillment of
the requirements for
the Degree of
DOCTOR OF PHILOSOPHY
May, 1987

A FOURIER TRANSFORM TO DETECT PINE SEEDLINGS IN A DIGITAL IMAGE

Thesis Approved:

Glenn Brambler
Thesis Adviser

Marvin Stone

Gerald Brusewitz

Donald D Fisher

Dan Yarbrough

Norman N. Durham
Dean of Graduate College

PREFACE

Each year, U.S. forest nurseries produce approximately 200 million pine seedlings. Forest companies depend on an adequate number of seedlings in order to replant timber land. To monitor the progress of seedlings, nurseries periodically conduct an inventory. The procedure is performed manually and is based on a statistical estimate. The process is slow, tedious, and imprecise. Automating the inventory procedure is subject of this dissertation.

A digital image processing technique to visually count pine seedlings is investigated. The technique is based on a proposed imaging system which resides on a platform behind a tractor. As the system passes over the seedling bed, image sensors capture an overhead view of individual seedlings. A computer analyzes the sensor values in order to detect and count individual seedlings.

This dissertation is concerned with developing a computer algorithm. Several test images were obtained. Pertinent seedling features in the images are gray level contrast, lines formed by the needles, and circular distribution of the needles. Four different techniques were investigated in an attempt to use these features to detect pine seedlings. These techniques are gray level peaks geometric intersection of needle lines, gray level

contour encoding, and a technique based on the Fourier transform.

The author wishes to express his appreciation to his major adviser, Dr. Glenn A. Kranzler, for his guidance and assistance throughout this study. This dissertation was made possible because of Dr. Kranzler's exceptional devotion, and I feel extremely fortunate to have studied under him. I would also like to extend a special thanks to committe member, Dr. Marvin Stone, for his guidance and assistance. Appreciation is also expressed to the other committee members, Dr. Gerald Brusewitz, Dr. Donald Fisher, and Dr. Rao Yarlagadda, for their invaluable assistance in the preperation of the final manuscript.

A note of thanks is given to Mr. Bill Boeckman and the Weyerhauser Corporation for permitting us to trample over a portion of their seedling bed in an effort to obtain photographs. I appreciated the efforts of Dr. Charles Tauer and Mr. David Gunther of the Forestry Department at Oklahoma State for providing invaluable assistance in growing and nurturing young pine trees. Thanks also go to Mr. Mark Appleman of the Agricultural Engineering Department for listening to some of the ideas which were a part of this dissertation.

Finally, my efforts would not have been complete without the loving support of my wife, Jan, and our one-year-old son, Matthew. These people kept me in balance thoughout the entire pursuit of this degree.

TABLE OF CONTENTS

Chapter		Page
I.	INTRODUCTION	1
	Applications of Digital Image Processing	1
	Statement of the Problem	7
	Value of the Study	10
	Objectives	11
	Limitations	11
II.	REVIEW OF THE LITERATURE	13
	Introduction	13
	Lines	13
	Edges	29
	Segmentation	34
	Edge Segmentation	34
	Threshold Segmentation	36
	Shape Recognition	43
	Internal Scalar Transforms	43
	External Scalar Transforms	45
	Internal Space Domain Techniques	49
	External Space Domain Techniques	55
	The Fourier Transform	65
	Fourier-Bessel Transform	66
III.	METHOD AND PROCEDURE	69
	Introduction	69
	Gray Level Peaks	70
	Geometric Line Intersections	72
	Contour Encoding	74
	Fourier Transform	76
	Implementation	91
IV.	ANALYSIS OF THE DATA	97
V.	SUMMARY AND CONCLUSIONS	102
	Summary	102
	Conclusions	104
	Recommendations for Further Research	107
BIBLIOGRAPHY		109

LIST OF TABLES

Table Page

1. Test Results 98

LIST OF FIGURES

Figure		Page
1.	A 1921 Digital Image	2
2.	Mature Seedling Nursery Bed	8
3.	Seedlings Shortly After Emergence	9
4.	Overhead View of a Seedling	14
5.	Basis Functions	18
6.	Freeman's Chain Code	20
7.	The Consecutive Singly Principle	23
8.	Three Quantization Schemes	26
9.	Spirographs	28
10.	Detecting Gray Level Peaks	42
11.	Fourier Descriptors	46
12.	Medial Axis	51
13.	Shape Matrices	54
14.	Extended Chain Codes	57
15.	A Syntactic Description	61
16.	Radial Symmetric Approximation	82
17.	Signal-to-Noise Ratio to Detect Seedling Center	84
18.	An On-Center Energy Spectrum	86
19.	An Off-Center Energy Spectrum	88
20.	A Seedling Image	89
21.	A Transformed Seedling Image	90

Figure Page

22. Maximum Energy Coefficient to Detect Seedling Center 92

23. Polar Coordinate Resolution 93

24. A Seedling Image Corrupted by Foriegn Objects . . . 95

25. Transform of a Seedling Image Corrupted by Foriegn Objects 96

26. A Missing Seedling 100

27. Detection Error 101

CHAPTER I

INTRODUCTION

Applications of Digital Image Processing

Digital imaging is not new. Perhaps the first digital image was produced in 1921, when the Bartlane picture transmission cable was introduced (Figure 1). A newspaper company used the cable to transmit pictures between London and New York. Images were coded into five distinct brightness levels and reproduced by a printer equipped with special type to simulate the brightness levels.

The benefits of digital image processing were not fully appreciated until the 1960's, during planetary exploration missions conducted by NASA. Close-up television pictures of the moon were made possible by the Ranger satellite (Hall, 1977). Images were transmitted to earth where they were digitized and then enhanced with the aid of a digital filter. Similar work continued during the Surveyor missions. In 1964, the first all-digital imaging system was launched on-board Mariner IV. Mariner's digital system sent clear images of Mars back to earth at the rate of 8 bits per second.

Source: McFarlane (1972)

Figure 1. A 1921 Digital Image

Developments in digital image processing continued during subsequent space missions. In 1977, Voyager II was launched. Analyzing digital images sent back by Voyager II helped to discover an unsuspected ring around Jupiter. Image processing techniques also yielded the first motion picture sequence of atmospheric changes on Jupiter (Jepsen et al., 1981). Enhanced images from Voyager II are revealing the first close-up images of Uranus (Gold, 1986).

Using a digital computer to process images requires a extraordinary amount of memory and speed. A single image could contain more than two million bits of information. If motion is important, a sequence of 30 images per second would require a processing rate of 63 million bits per second.

In the past, computer memory and processing speed limited the number of applications for image processing. A computer capable of the computational task was physically too large to be practical in many situations. Moreover, the cost of such computers prohibited many applications. Until the past few years, image processing was constrained to a few specialized areas, such as space exploration. However, computer processing capabilities have not been stagnant.

Recent technological developments in the manufacturing of semi-conductor devices have provided microcomputers with both the processing speed and memory to analyze images. Cost for microcomputer-based systems is in the tens of thousands of dollars. In industries which require product inspection,

capital investment for vision inspection systems is offset by increased productivity. Payback periods can be as short as four months (Wagner, 1983). Consequently, several industries have already begun to implement vision technology on the production line.

General Motors Corporation is using an image-based system to aid in assembling valve spring keys (Dodd, 1983). The system, called Keysight, is being used to detect the presence of keys which retain valve spring assemblies in engine blocks. Human inspectors had no room for error. A missing key would ruin the engine since the valve would eventually drop into the combustion chamber. Machine vision provided a more reliable alternative.

General Electric is using a camera to inspect plastic bottles (Mayo, 1982). A typical defect that occurs when molding plastics is a moil (an extraneous piece of plastic attached where the two halves of the mold come together). The machine vision system detects moils and automatically rejects defective bottles.

Westinghouse robots are using machine vision (Kinnucan, 1983). A camera-guided robot arm places metal slugs in a mold for forming turbine blades. The camera then inspects the final blade for defects before further assembly.

Food industries are also exploiting the benefits of digital imaging. A vision system is being used to inspect frozen pizza crusts (Hudson, 1984). Image data are analyzed to determine if the crust has holes, cracks, or burn spots. If the computer

"sees" a defect, it activates an pneumatic solenoid which automatically removes the defective crust from the product line. About 200 crusts per minute are inspected.

Chocolate coated candies are being checked for voids in the coating (Hudson, 1984). When the coating cools, air bubbles are sometimes trapped on the bottom, causing an undesirable appearance. Images of the bottom surface are analyzed to detect the chocolate craters. Two pieces of candy are examined every second.

French fry strips are being inspected by a system produced by Key Technology, Inc. (Kranzler, 1985). The system coordinates the action of water-activated knives to remove discoloration defects. Production rates of 9070 kg (20,000 lb) per hour have been achieved.

There are many examples of machine vision in industry. Advances in computer performance will increase the number of applications. In fact, many experts estimate the machine vision industry is still in its infancy (Frost and Sullivan Inc., 1986).

Perhaps the newest area of vision technology is a direct consequence of computer portability. Computers capable of processing images can be made portable to the extent of in-field operation. Research has already begun to investigate several in-situ possibilities.

Cucumber growth has been monitored by a vision system in Japan (Eguchi et al., 1979; Eguchi and Matsui, 1977; Eguchi and Matsui, 1978). Plant vigor was determined to be a function of size and near-infrared spectral reflectance. Three orthogonal camera views were used to photograph the plants. Size was determined from image area. Geometric measurements of plant growth have also been studied by Meyer and Davison (1985) and DaSilva et al. (1985).

Baylou et al. (1983) have investigated a two-camera system to automate asparagus picking. Asparagus mounds are backlit to enhance contrast. While in motion, the computer analyzes several images in order to calculate the position of each plant. Mechanical harvesting is performed by a robot arm.

Automatic harvesting of tomatoes (Whittaker et al., 1984), oranges (Harrel et al., 1985), and apples (Grand d'Esnon, 1984) are other possible applications which exploit vision systems.

The use of image data to automatically guide field equipment is being studied (Reid and Searcy, 1986; Searcy ; Gerrish and Surbrook, 1984). Row crops form lines which create a unique perspective that enables an on-board computer to calculate the vehicle's direction. A sequence of images is analyzed to continuously steer the vehicle.

These are only a few of the agricultural applications of vision technology. Further study in this area should provide some interesting new tools for agriculture.

Statement of The Problem

About two hundred million pine seedlings are produced in U.S. forest nurseries each year. Annual income from these seedlings is approximately two million dollars. In Oklahoma, seeds are planted in March, and by December young trees are ready for shipment (Figure 2). Not all seeds produce salable plants, however. Some seeds do not germinate. Insects, weeds, and adverse weather conditions can also reduce the number of usable seedlings.

In order to ensure enough seedlings are produced, the seedlings are periodically counted during the growing season. One of the most important counts is taken shortly after emergence of the young seedlings (Figure 3). The emergence count is critical because germination failure is the major factor affecting seedling mortality. In fact, many nursery managers expect only about 80 percent of the seedlings will germinate. In addition to the emergence count, counts are taken during the growing season to monitor the progress of the plants. These later counts are useful in making economic projections. In a sense, seedlings in the field are unsold products in inventory. In any business, accurate inventory control is vital to economic efficiency.

Current inventory practice is based on statistical sampling. A section of the seedling bed is selected at random and the seedlings within the section are counted by hand. This

Figure 2. Mature Seedling Nursery Bed

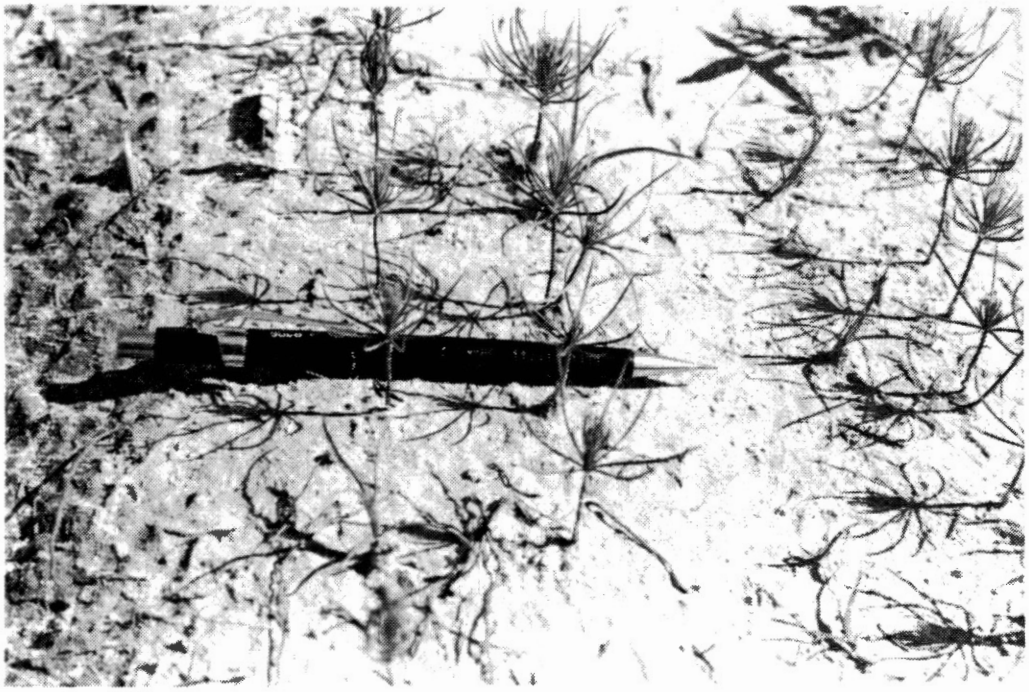

Figure 3. Seedlings Shortly After Emergence

procedure is repeated and the counts are used to statistically estimate the total seedling population. The sampling procedure is time consuming and estimates are often accurate to within only ± 15 percent (Boeckman, 1986). Automated inventorying techniques are being sought by the seedling industry.

Value of the Study

This dissertation is concerned with developing a technique to automate seedling inventorying. A digital image processing system that is capable of counting pine seedlings will permit a timely and accurate estimate of the number of seedlings growing in the field. Accurate estimates of the population would ensure the status of the crop and thus improve the efficiency of marketing the seedlings.

The capability of an image system to recognize different objects may be useful for production of row crops in general. For example, an image system could be mounted on a platform behind a tractor. As the tractor is driven over the field, image sensors aimed at the seedling bed continuously transfer digital data to several concurrently running algorithms. One algorithm detects the crop plant and maintains statistics on the health of the crop with respect to field position. Another algorithm recognizes a certain type of weed and automatically triggers the application of a controlled amount of herbicide. In a similar manner, pesticides are precisely applied. The image system enables the conditions of the crop to be more closely monitored,

and the selective application of pesticides and herbicides would reduce production costs.

Objectives

The objective of this dissertation is to develop a digital image processing technique to detect and count pine seedlings. Efforts are focused on developing a mathematical procedure. The objective can be subdivided into three parts:

1. Develop an algorithm to detect individual pine seedlings in a digital image.

2. Implement the algorithm on a digital image image processing system.

3. Demonstrate the capability of the particular implementation to count pine seedlings.

Limitations

Certain limitations have been imposed so that efforts can be focused on the specific objective. Most limitations are concerned with emphasizing the development of an algorithm, and avoiding issues which tend to be system dependent.

Testing the algorithm will be performed in the laboratory under controlled environmental conditions. Images will be obtained from seedlings grown in four trays (30 cm X 60 cm). The camera will be positioned approximately one meter above the seedlings, looking directly downward.

The condition of relative motion between camera and ground will not be addressed. An image of an object in motion can be acquired by using a line-scan sensor. Different lines in the image are obtained by a slight displacement perpendicular to the direction of travel.

The soil in each tray will contain a high percentage of organic content. Incandescent lighting will be used to illuminate the seedlings. This particular combination is successful at achieving high contrast, since the wavelengths of maximum light energy matched the peak sensitivity of the camera (CCD sensor), and the albedos of the plant and soil are very different in this range (0.7 to 1.3 μm).

The seedlings will be tested about four weeks after emergence. At three to four weeks, the tips begin to elongate and seedling features are easily distinguished.

Computer processing time of the specific software implementation will not be a primary concern. Processing time is a system dependent variable. When processing time is a concern, an algorithm can usually be implemented in hardware which can decrease execution time by several orders of magnitude.

Reader knowledge of digital image processing terminology and commonly used functions will be assumed.

CHAPTER II

REVIEW OF THE LITERATURE

Introduction

From an overhead view, pine seedlings appear to have three distinctive features (Figure 4). The most predominate feature is lines generated by the pine needles radiating outward from the seedling's center. Another feature is gray level difference. With proper contrast, the center of the seedling always has a different gray level than the surrounding soil. The third feature is the approximate circular distribution of needles.

These three features form the basis of the literature review. Needles prompted an investigation of literature pertaining to lines. The gray level contrast motivated research dealing with segmentation techniques. Distribution of the needles in a circular shape led to a study of algorithms for shape analysis. Finally, two commonly used image transforms are described.

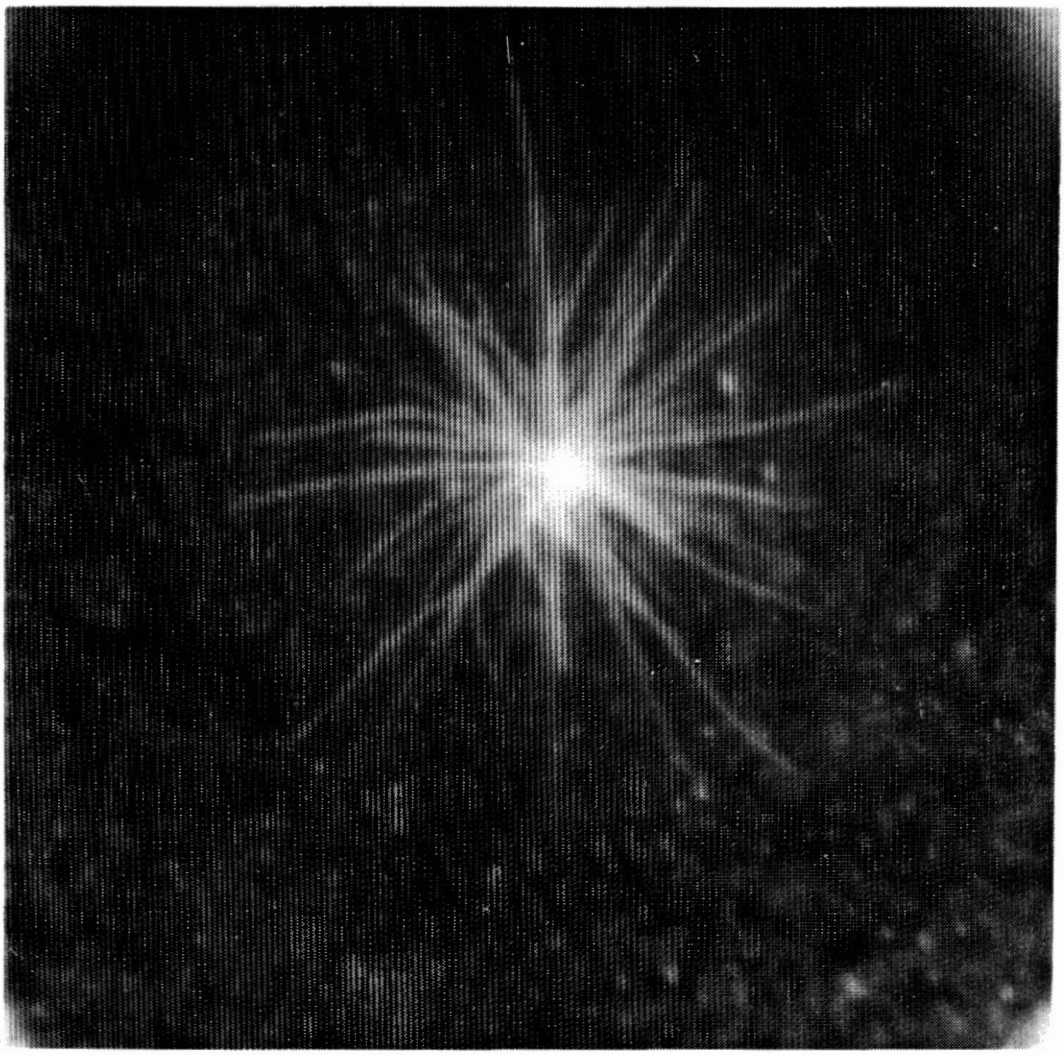

Figure 4. Overhead View of a Seedling

Lines

Objects appearing in natural scenes usually have distinct boundaries. In a picture of a natural scene, boundaries appear as either edges or lines. Detecting the position and orientation of a line is a fundamental task in object recognition.

A line in a digital image consists of pixels which meet certain requirements. Rosenfeld and Thurston (1971) defined two conditions for a point which lies on a line:

> 1. It has a pair of lower valued neighbors on opposite sides of it (in the direction across the curve).
>
> 2. It has two other neighbors (in the direction along the curve) which satisfy 1.

The conditions listed above pertain to white lines on a black background. The converse holds true for black lines on a white background. Zucker et al. (1975) identified the same two conditions for classifying points on a line.

One method of detecting the lower-to-higher-to-lower transition is linear filtering (Deutsch, 1966; Pratt, 1978; Gonzales and Wintz, 1977). Lines of unit width are detected by convolving the image with the matrices,

$$\mathbf{V} = \begin{bmatrix} -1 & 2 & -1 \\ -1 & 2 & -1 \\ -1 & 2 & -1 \end{bmatrix} \qquad \mathbf{H} = \begin{bmatrix} -1 & -1 & -1 \\ 2 & 2 & 2 \\ -1 & -1 & -1 \end{bmatrix} \tag{2-1}$$

Positive values from $\mathbf{V}$ indicate possible vertical lines; likewise, $\mathbf{H}$ indicates possible horizontal lines. Similar matrices can be used to detect diagonal lines. Linear filtering is a commonly used technique, but it has a major drawback.

Linear filtering may be unable to distinguish between lines, edges, and spots. For example, depending on the magnitude of gray level difference, the output from $_V$ could be the same for a line, edge, or spot. As Rosenfeld and Thurston (1971) state,

> This [the output from V] will have output 3k when in register with a vertical line segment whose gray level is k greater than the background; but it will have the same output for a single point whose gray level is 3k greater than the background level, or for a vertical edge between gray levels which differ by 2k.

A Boolean test for lower-to-higher-to-lower pixel magnitude avoids the ambiguity in distinguishing between lines, edges, and spots. Linear filtering is perhaps the simplest approach to line detection.

A statistical approach to line detection was presented by Griffith (1973a). Griffith's algorithm uses the probability density function to calculate the probability of a line occurring along a narrow band between two specified points. A threshold probability is used to decide if a line exists between the two points. The statistical approach successfully detected lines in noisy images. In particular, the algorithm performed well when a change in background luminescence was present between the two points.

A more classical approach to line detection was introduced by Hueckel (1973). The theory of Hueckel's approach was originally introduced to detect edges (Hueckel, 1971). Later, the idea was expanded to detect lines. Hueckel's principal

contribution was the discovery of a unique set of Cartesian basis functions which can be used to recognize patterns in a circular subset of an image, which Hueckel calls D. Hueckel states . . .

> The set of all real functions over D is a Hilbert space. Every pattern such as the edge, the line, edge-line, the dot, the checkerboard, the letter A, or a certain person's face occupies a characteristic subspace E. E is the set of all ideal (i.e. unperturbed) instances of the pattern.

The basis functions are selected so that the Hilbert vector representing E is a Fourier spectrum. The basis functions are products of angular and radial wave functions. Determining their frequency spectra reduces to Fourier analysis in polar coordinates. Figure 5 shows all nine basis functions. The zero crossings of each basis function are at every perimeter, and at any interior circle or line. Each function produces a coefficient from the input data (the pixel values within D). From the coefficients, a number is calculated which measures how closely the input data match an ideal pattern. The number representing the match is compared with a threshold to decide if the particular input pattern contains the ideal pattern.

Hueckel points out that the key to the algorithm's success is limiting the number of basis functions to nine. Holding to nine basis functions greatly simplifies the computational task, because determining the optimum match vector can be explicitly pre-solved. The Hueckel operator requires approximately 23 arithmetic operations per pixel point.

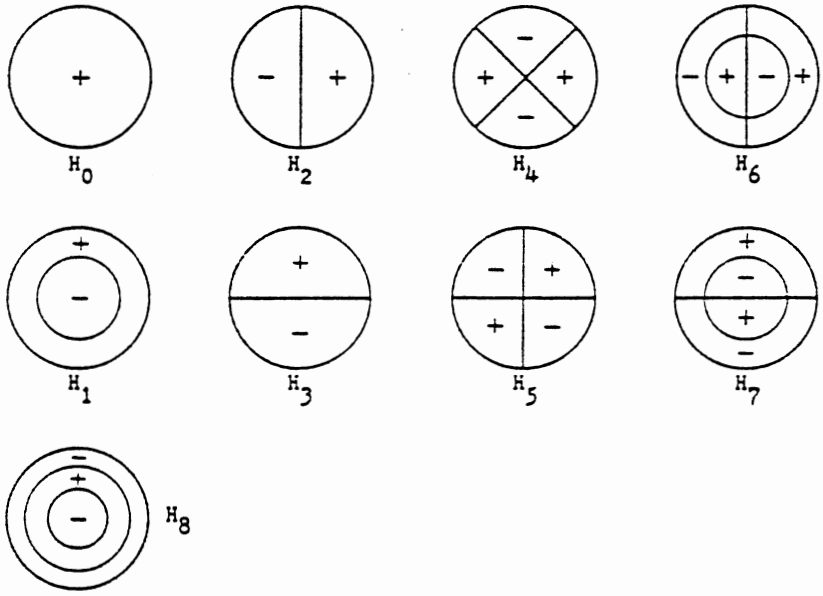

Source: Hueckel (1973)

Figure 5. Basis Functions

Determining regions which contain line segments is only part of the problem of identifying a line in a digital image. Another computation involves feature extraction. In other words, given the pixel coordinates of points on a line, what can be determined about the pose of the line.

The fundamental aspect of feature extraction is that the data obey some rule characteristic of the feature. For example, points on a line obey the slope-intercept rule. In fact, a way of using the slope-intercept rule to detect lines has been patented (Hough, 1962).

The most common approach to identifing lines is based on an idea introduced by Freeman (1961). Freeman originally introduced the idea of encoding arbitrary geometric curves. The established method of curve encoding was to record the coordinates of each point. As Freeman points out, "If the points describe a continuous curve, they are, of course, far from independent." He continues to describe what is now known as the chain-code. Nearly all present-day line encoding schemes are based in some way on the chain-code.

The chain-code exploits the fact that if one point on a curve is known, the adjacent point can assume one of eight possible directions (for a rectangular grid). If the decimal digits zero through seven are assigned to each of these directions, any curve can be described as a sequence of three-bit directional codes (Figure 6).

(a)

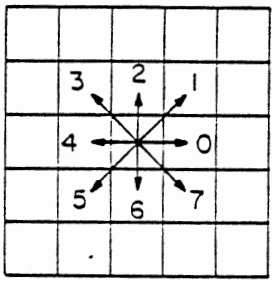

(b)

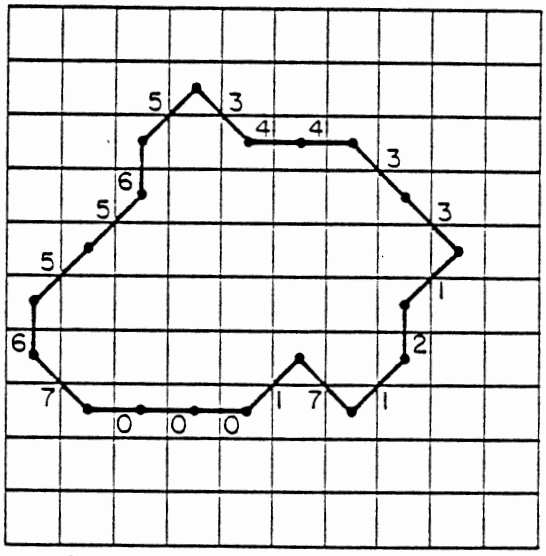

Chain encoding of boundary lines

CHAIN CODE:

00017 12133 44356 5567

Source: Pratt (1978)

Figure 6. Freeman's Chain Code

Freeman continues to discuss several interesting properties of the chain-code. Adding "2" (modulo 8) to each of the digits in the code rotates the curve 90 degrees in a counter-clockwise direction. Similarly, subtraction causes a clockwise rotation. Expansion, or magnification of the curve, is achieved by replacing each code digit by N identical digits, where N is an integer representing the expansion ratio. Curve length is found by counting the number of even digits plus the square root of two times the number of odd digits. Other procedures for determining closure, intersection, and enclosed area are also presented.

The chain-code of a digital line has three properties which are generally accepted as necessary conditions for a line (Freeman, 1970). They are:

> 1) at most, only two directional codes are present which can differ only by unity, modulo 8,
>
> 2) one of the two directional codes always occurs singly,
>
> 3) successive occurrences of the directional code occurring singly are as uniformly spaced as possible.

While the third criterion remains somewhat "fuzzy", formal proof of the first two criteria was presented by Rosenfeld (1974a), and later by Gaafar (1977). Rosenfeld based his proof on an idea he calls the chord property. Rosenfeld states that a digital arc is the digitization of a straight line segment if, and only if, it has the chord property. The chord property has been paraphrased as follows. Let pq be a real line segment

between points p and q, and let S represent the digital arc approximating pq. S has the chord property if, for every point (i,j) in S, there exists a point (x,y) on pq such that the maximum of (i-x), (j-y) is less than one.

Kim and Rosenfeld (1982) and Kim (1982) used the chord property to show how digital straight line segments can be used to define convex regions. They define a digital region as convex if, and only if, every pair of points in the region is connected by a digital straight line segment contained in the region. The mathematical basis of the chord property leads to the development of some useful line detecting algorithms.

Wu (1980, 1982) developed an algorithm useful for determining if a particular chain code represents a line. The algorithm is based on an idea called the consecutive singly (CS) principle, which is essentially Freeman's first two requirements, i.e., the chain code of a line has at most two consecutive symbols (modulo 8) and one of these symbols occurs singly. Wu's algorithm repeatedly restructures the chain code of a line. An example is shown in Figure 7. Each digit of level two is the number of digits comprising a run in level one (the directional code digit which occurs singly is ignored). The restructuring process is repeated for higher levels until either the CS principle is violated, or a level is obtained with a single digit. If a single digit is obtained, the original sequence represents a straight line. Some of Wu's ideas have been refined in a later

Chain Code =	1	0	1	0	1	0	1	0	0	1	0	1	0	1	0	0	1	0	1	0	1	0	0
Level 2		1		1		1		2		1		1		2		1		1		2	
Level 3				3								2						2			
Level 4														2							

Source: Hung (1985)

Figure 7. The Consecutive Singly Principle

paper by Hung (1985). The chord property is not without some limitations.

Lee and Fu (1982) recognized the problem of applying the ideal mathematical theory of the chord property to real-world images. As Lee and Fu state:

> While the chord property is concise and rigorous, it is often too restrictive for the determination of straight lines in practical applications. Many digital arcs obtained from edge detection operations on real images of straight lines do not have this ideal property, either because of unexpected disturbances or because of the arcs being the boundaries of solid objects.

Lee and Fu used the Fast Fourier Transform (FFT) to detect the periodicity of a chain code sequence. The chain code sequence is transformed into the frequency domain. The frequency of maximum amplitude is compared with the average period of the chain code. If the difference is less than a predefined threshold, the chain code represents a line.

Another approach using the chain code to describe a straight line is linguistic parsing (Knoke and Wiley, 1967; Feder, 1968; Leroi and Burton, 1980; Fu, 1982a). Brons (1974) used syntactical pattern recognition to develop an algorithm which is similar to the chord property (Arcelli and Massarotti, 1975). Brons presents several different grammars and deals with the case when noise is added in the digitization sequence. Syntactic pattern recognition is discussed in more detail later in this chapter.

The chain code is a digital approximation of a continuous curve or line. As in any quantizing process, there is a certain amount of error inherent in the chain code of a curve or line. Groen and Verbeek (1977) have discussed the accuracy in using Freeman's chain code to approximate contours. They used the probability density function to estimate errors in curve length and degree of curvature created as a result of approximating a digital contour using Freeman's chain code.

Dorst and Smeulders (1984) derive a mathematical expression for the set of all continuous line segments which could have generated a given chain code string. In addition, the relationship to the chord property is briefly discussed.

Koplowitz (1981) has presented a comparison of three different chain code schemes. The three encoding schemes are based on: 1) a square quantization, 2) a circular quantization, and 3) grid-intersect quantization (Figure 8). The square quantization scheme is the familiar Freeman chain code. The circular grid uses the nearest point within a specified radius. The grid-intersection method selects discrete points based on the intersection of the curve with grid lines (a type of "stair-step" encoding scheme). Koplowitz compares each scheme based on the number of bits required to encode a given curve, and error (in a least squares sense) in curve direction and length.

Saghri and Freeman (1981) generalize Koplowitz's results by showing that the precision of a chain code is based on the size or resolution of the underlying grid and not on the form of the

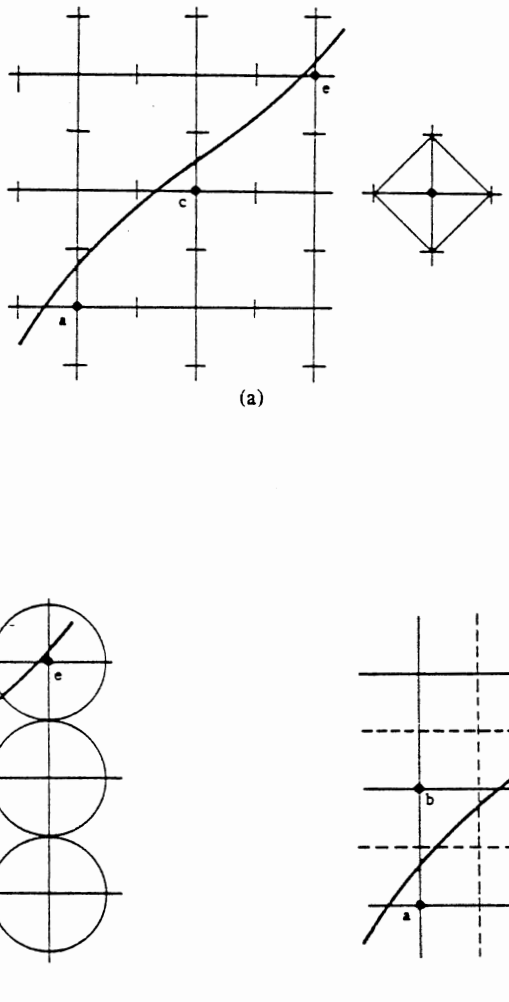

Source: Koplowitz (1981)

Figure 8. Three Quantization Schemes. (a) square. (b) circular (c) grid-intersect.

code.

A recent development which makes use of Saghri and Freeman's basic conclusion is the multiple-grid (MG) code (Minami and Shinohara, 1986). The MG code uses two points on each side of a pixel instead of the corners used by Freeman's code. Minami and Shinohara have also incorporated the Huffman code to improve coding efficiency. The Huffman code exploits the frequency of occurrence to minimize the number of bits required to encode a particular numerical sequence (Huffman, 1952). Minami and Shinohara demonstrate a 60-70 percent improvement in coding efficiency over the Freeman code. They also claim that ". . . the subjective quality of the regenerated line drawings by this algorithm is excellent."

A graphical technique representing the quantization error in the chain code of a line has been presented by Dorst and Duin (1984). The technique produces graphs called spirographs, named after a child's toy used to create polygon drawings. The spirograph of the line shown in Figure 9a is illustrated in Figure 9b. Spirographs are specific for a given line slope and number of digital points used to quantify the line. The points on the circumference of the spirograph represent the relative position of changes in the chain code caused by errors in the intercept. For example, if the y-intercept of the dark line in Figure 9a is gradually increased, no change in the chain code occurs until the line intersects the grid point of column two (assuming a grid-intersection quantization scheme). The next

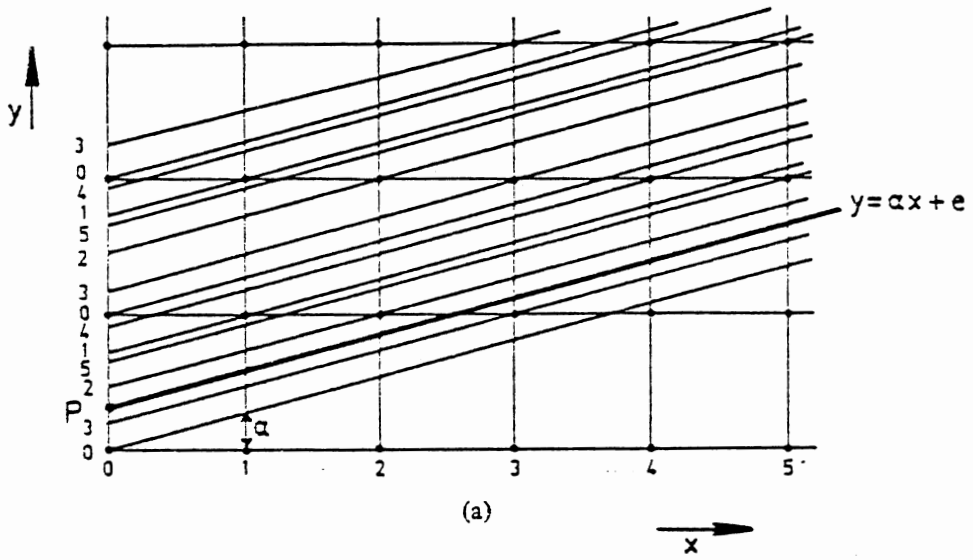

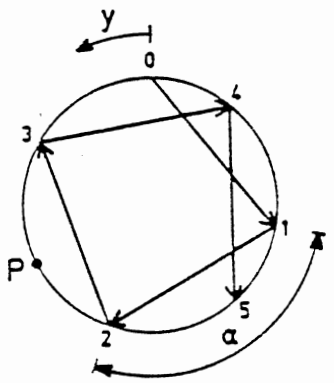

Source: Dorst and Duin (1984)

Figure 9. Spirographs. (a) multiple chain-code lines. (b) the spirograph.

change occurs when the line intersects column five. From the sequence along the circumference of the spirograph, intersections occur in column one, four, zero, three, and the sequence repeats beginning with two. The positional inaccuracy of a point in a chain code is indicated by the relative position of the point on the circumference of the spirograph. Dorst and Duin use spirographs to develop theorems relating digitized straight lines to elementary number theory (Farey series, continued fractions).

Lines are closely related to edges. Edges are often used to generate artificial lines for three-dimensional object recognition. Edge matrices are used to detect edge points which are spatially combined to generate a line (Nevatia, 1976; Robinson, 1976; Mero, 1981). The perspective orientation of lines defining an object's boundary can be used to reconstruct the three-dimensional shape of the object (Roberts, 1965; Griffith, 1973b).

Edges

Edge detection is one of the most important parts of image segmentation leading to interpretation (Marr, 1975). There are many different techniques of detecting an edge in a digital image. Davis (1974) and Hildreth (1985) have provided a survey of the more popular edge detection algorithms.

For a human, the process of detecting edges seems deceptively simple. Research suggests that edges in a visual scene may be detected by the retina before reaching the brain (Hubel and Weisel, 1962). The significance of edge detection may elude the human brain, because edges have already been identified and appear as an integral part of the entire scene.

Jacobs and Chein (1981) have developed an edge enhancement technique based on a biological analogy. Their paper also includes an excellent comparison of several commonly used edge-finding algorithms.

One of the first methods for detecting edges with a digital computer was proposed by Roberts (1965). An image, **F**, with a gray level denoted by f(i,j) at point (i,j) has an edge image, **G**, calculated from,

$$g(i,j)=\sqrt{[f(i,j)-f(i+1,j+1)]^2+[f(i,j+1)-f(i+1,j)]^2} \qquad (2\text{-}2)$$

Robert's technique is somewhat susceptible to noise, since only four points are involved in any one calculation.

Spatial differentiation is another edge enhancement procedure (Pratt, 1978). The first-order derivative is approximated by subtraction in the discrete domain. Horizontal edges could be calculated from,

$$g(i,j) = f(i,j) - f(i,j+1) \qquad (2\text{-}3)$$

and vertical edges from,

$$g(i,j) = f(i,j) - f(i+1,j) \qquad (2\text{-}4)$$

Second-order differentiation is accomplished simultaneously for both directions by performing a convolution of the image with Laplacian matrices. Examples of three Laplacian matrices are shown below.

$$\begin{bmatrix} 0 & -1 & 0 \\ -1 & 4 & -1 \\ 0 & -1 & 0 \end{bmatrix} \qquad \begin{bmatrix} -1 & -1 & -1 \\ -1 & 8 & -1 \\ -1 & -1 & -1 \end{bmatrix} \qquad \begin{bmatrix} 1 & -2 & 1 \\ -2 & 4 & -2 \\ 1 & -2 & 1 \end{bmatrix}$$

The degree to which an image is enhanced by a Laplacian matrix can be made proportional to the statistical correlation of pixel values (Pratt, 1978). The correlation matrix is defined by,

$$\begin{bmatrix} P_c P_r & -P_c(1+P_r^2) & P_c P_r \\ -P_r(1+P_c^2) & (1+P_c^2)(1+P_c^2) & -P_r(1+P_c^2) \\ P_c P_r & -P_c(1+P_r^2) & P_c P_r \end{bmatrix}$$

where P_c and P_r represent the correlation coefficients between columns and rows, respectively. In the case of no correlation, P_c and P_r would be 0 and the convolution would have no effect on the image. Perfect correlation would occur when $P_c=P_r=1$. In this case, the matrix reduces to a Laplacian.

Another commonly used edge detection scheme is the Sobel operator (Duda and Hart, 1971). The idea is to use two, 3x3 matrices which are defined as follows:

$$\mathbf{V} = \begin{bmatrix} -1 & 0 & 1 \\ -2 & 0 & 2 \\ -1 & 0 & 1 \end{bmatrix} \qquad \mathbf{H} = \begin{bmatrix} 1 & 2 & 1 \\ 0 & 0 & 0 \\ -1 & -2 & -1 \end{bmatrix}$$

Letting X equal the convolution result of V and Y equal the result of convolving with H, the gradient value, g(i,j), is calculated from,

$$g(i,j) = \sqrt{(X^2+Y^2)} \qquad (2\text{-}5)$$

Kirsh (1971) has introduced a difference operator which works in several directions, the maximum value being taken as the gradient. The enhancement is given by,

$$g(i,j) = \text{MAX}\left[1, \underset{i=0}{\overset{7}{\text{MAX}}}\left[\left| 5S_i - 3T_i \right| \right] \right] \qquad (2\text{-}6)$$

where,

$$S_i = A_i + A_{i+1} + A_{i+2} \qquad (2\text{-}7)$$

$$T_i = A_{i+3} + A_{i+4} + A_{i+5} + A_{i+6} + A_{i+7} \qquad (2\text{-}8)$$

The subscript are evaluated using modulo 8 arithmetic. The A_i's refer to coefficients in the convolution matrix,

$$\begin{bmatrix} A_0 & A_1 & A_2 \\ A_7 & f(i,j) & A_3 \\ A_6 & A_5 & A_4 \end{bmatrix}$$

A logarithmic transformation might be useful when multiplicative changes in luminous level exist in an image (Pratt, 1978). The difference of the logarithm of a pixel and the average logarithm of its 4 nearest neighbors is compared to a preset threshold value. The gradient calculation is described by,

$$g(i,j) = \frac{1}{4} \text{LOG}\left[\frac{f(i,j)^4}{A_1 A_3 A_5 A_7} \right] \qquad (2\text{-}9)$$

Rosenfeld (1970b) has developed a method which uses a nonlinear product averaging procedure. The one-dimensional gradient is calculated from,

$$d(i,j) = \frac{1}{M}[f(i+M-1,j) + f(i+M-2,j) + \ldots + f(i,j) - f(i-1,j) - f(i-2,j) - \ldots - f(i-M,j)] \quad (2\text{-}10)$$

where $M = 2^k$, and k is an integer. Values for d(i,j) are calculated up to some predetermined limit of k. The gradient value is then determined by multiplying all the d(i,j) values. The product is maximum only when all components are maximum. Large values of M detect major edges while smaller values correspond to edges with smaller magnitude.

Tabatabai and Mitchell (1984) use a process to locate edges to subpixel values (subpixel means the edge location need not be a sampled pixel point). The technique is introduced by using a one-dimensional edge, and later extended to work in two dimensions. An edge represented by a step function is positioned so as to preserve the first three sample moments. Sample moments are defined as,

$$m_i = \frac{1}{n} \sum_{j=i}^{n} x_j^i \; ; \; i=1, \; 2, \; 3 \quad (2\text{-}11)$$

where x_j represents discrete input values. Sample moments are invariant under scaling and translation. Tabatabai and Mitchell compare the performance of their edge algorithm with the Hueckel

(1973) and Sobel (Duda and Hart, 1971) operators in the presence of Gaussian noise.

Segmentation

Segmentation is the division of an image into regions which posses a similar attribute. Fu and Mui (1981) have provided a survey on image segmentation techniques. The most common attribute used to segment an image is pixel luminescence. Two techniques which use pixel light intensity are edge detection and gray level thresholding.

Edge Segmentation

The Sobel edge detector was used by Perkins (1980) to segment images into regions of similar intensity. Perkins used an edge relaxation technique to bridge gaps in the boundary of an object. Relaxation is a multi-pass operation which detects more subtle edges on subsequent passes (Rosenfeld, 1978). Correspondingly, subsequent passes are localized to an area where gaps are present in the original boundary. Regions enclosed by a boundary define separate objects.

A different relaxation procedure was used by Danker and Rosenfeld (1981) to segment images into regions called "blobs". As they defined it, "A blob is a compact region lighter or darker than its background surrounded by a smoothly curved edge." A local neighborhood is used to recursively calculate the probability that only one region is present. Probabilities

indicating more than one region identify boundaries. The calculation is based on the results of the previous iteration as well as the values of the current neighborhood. The process runs in parallel and can be repeated to detect more subtle boundaries.

Minor and Sklansky (1981) used Sobel matrices to segment an image. Raw images are preprocessed using an intensity normalizer to equalize the contrast range to 256 gray levels. The normalized images are filtered by subtracting an average gray level obtained from a 17 by 17 pixel neighborhood. The high frequency results are used as input to the Sobel edge detector. Edge points are combined in a spoke filter (a variation on the Hough transform, which is defined later in this chapter) to detect objects in the original image. Examples show detection of military tanks and armored personal carriers.

Gradient values are used to determine boundaries in the bead chain algorithm (Gritton and Parrish, 1983). Convex regions with smooth boundaries are approximated by ideal geometric figures (circle or an ellipse) having the same center. Boundary pixels of the ideal figures are adjusted in a radial direction from the center so as to maximize the local gradient. The algorithm uses an a priori knowledge of the object's shape to segment the object from the background. Testing of the bead chain algorithm was performed on electron micrograph images of liver cells. Individual mitochondria were successfully detected in extremely noisy images.

Sarkar and Wolfe (1985) used Robert's gradient to detect scars on the surface of tomatoes. Segmentation was accomplished by using syntactic pattern recognition to recognize strings possibly indicating the boundary of a scar. Another commonly used technique to segment an image is gray level thresholding.

Threshold Segmentation

A survey of thresholding algorithms has been provided by Weska (1978). In general, the thresholded image, **G**, can be described as a function,

$$g(i,j) = t(i, j, n(i,j), f(i,j)) \qquad (2\text{-}12)$$

where n(i,j) is a local operator around the point (i,j), and other symbols are as previously defined. In the simplest case, the function depends only on f(i,j). All pixels smaller than some predefined value are classified as background; all pixels greater than, or equal to, the value are classified as object. The result is a binary image. The same action is taken over the entire image, hence the name global thresholding.

Selecting the threshold level is crucial to the success of global thresholding. One simple approach is to use human interpretation to qualitatively determine a threshold level. Sistler et al. (1982) used this method to analyze droplet size distribution of various agri-chemicals. Berlage et al. (1984) used the same approach to distinguish between crop seeds and their contaminants.

Selecting a threshold level by human interaction defeats some of the advantages of machine vision. In an industrial application, manually selecting a threshold value takes time and would reduce productivity. In addition, human decisions based on visual appeal are qualitative, and may be different for different people.

Most procedures for thresholding an image are based on a quantitative calculation. One of the first automatic threshold selection algorithms was described by Doyle (1962). The process was based on the histogram of the image, which indicates the number of pixels at each gray level. The threshold level, t, was selected so that a specific percentage of the pixels in the image was greater than t.

Using the histogram's shape was probably first proposed by Prewitt and Mendelsohn (1966). White blood cells were segmented by locating peaks in a bimodal histogram of the image. One peak occurred at a gray level corresponding to the background; the other corresponded to the white blood cells. The antimodes or "valleys" of the histogram indicated the threshold gray level. Successful segmentation usually requires smoothing of the histogram data.

Guyer et al. (1984) used a classical approach to global thresholding. Plants are segmented from a soil background in an attempt to identify shape. The image is assumed to have two principal brightness values, each containing a certain amount of additive Gaussian noise. The probability density function is

used to calculate the minimum-error threshold level. Derivation of an expression for the threshold value based on the probability density function can be found in the book by Gonzales and Wintz (1977). Feivson (1983) has also used the probability density function to segment satellite images of different forest land.

Most present day real-time applications use global thresholding. Processing time is minimal, and the operation can be simultaneously performed over the entire image array. The liability of global thresholding is the stringent demand on lighting.

Successful segmentation using a global threshold requires a high degree of contrast. Contrast is usually achieved by lighting objects from behind (Baylou et al., 1983). However, artificial lighting is not always possible, and even if it is possible, luminous levels are rarely uniform over the entire image. Global thresholding may successfully segment a blob from the background, but slight changes in the background level will bias the binary representation. The limitations of global thresholding have prompted investigation of more sophisticated algorithms.

The bimodal histogram technique can be enhanced using a local pixel difference to calculate a threshold value (Weska, 1978). Each pixel is weighted in the histogram according to the difference between the pixel's value and the average of a local region. Small differences receive more weight than large

differences. The result is a histogram with deeper valleys, thus reducing the likelihood of error in threshold selection.

Second-order differences can also improve the bimodal selection scheme (Weska et al., 1974). The Laplacian convolution is used to detect pixels which locate regions of quadratic change in gray level. Quadratic change occurs at either end of the transition from background to object. The position of pixels having large values from the Laplacian are used to locate pixels in the original image. Only these pixels from the original image are used to form the histogram. As a consequence, the histogram has a more equal number of pixels between object and background. The bimodal selection procedure is less prone to error than when performed on a simple histogram, which usually reflects a condition where more pixels represent the background than object.

Dondes and Rosenfeld (1982) use an idea called "local busyness." Local busyness is calculated from,

$$b(i,j) = \text{MIN}[\ |A_0-A_1| + |A_1-A_2| + |A_7-f(i,j)| + |f(i,j)-A_3| + |A_6-A_5| + |A_5-A_4| \qquad (2\text{-}13)$$

Subscripts of A are defined in equations 2-7 and 2-8. An algorithm to smooth images from the busyness values is presented. The idea is to reduce areas of high busyness so that a more confident estimate of the object's gray level can be obtained.

Bartz (1969) described a method to threshold images of printed characters for optical character recognition. The procedure uses a combination of four threshold levels which are calculated by assuming a linear relationship for certain observed distortions. As an example, a threshold to respond to contrast distortion might be calculated from,

$$T = B_0 + B_1K \qquad (2\text{-}14)$$

where K is the average contrast over previously scanned characters and B_0 and B_1 are empirically selected optimizing parameters.

Situations where the background luminescence changes usually require dynamic thresholding. Dynamic thresholding takes into consideration the position within the image, as well as the results of operations on neighboring pixel values, in order to calculate a threshold level.

Chow and Kaneko (1972) employed dynamic thresholding to segment radiographic images. A 7 by 7 window centered at each point is used to calculate a histogram and its variance. From the histogram and variance, a threshold level was determined for each point in the image. A linear interpolation combined the threshold value at each point to achieve a continuously varying threshold over the entire image.

Recursive region splitting is another commonly used dynamic thresholding technique (Shneier, 1983). Hong and Rosenfeld (1984) describe a recursive technique based on a tree

data structure. Each node represents a certain gray level variance calculated over a region. The regions are subdivided into smaller regions which are represented as children of the parent node. The variance is used to indicate when a region is uniform, thus representing a single object (or background). In addition to variance, edge information within each region can also be used (Hong and Shneier, 1984). A similar decomposition technique is described by Ohlander et al. (1978).

Segmentation is only one application of recursive region splitting. The data structure used in region splitting is called a quadtree. Several additional references are available to the interested reader (Rosenfeld, 1980; Ranade and Shneier, 1980; Samet, 1984; Samet and Webber, 1984; Klinger, 1984).

One interesting application using quadtrees is detecting gray level peaks (O'Gorman and Sanderson, 1984). A square image of size (nXn) is partitioned into four overlapping squares of size (n-1)X(n-1) (Figure 10). The sum of pixel values within each square is calculated. The square having the largest value is selected to repeat the partitioning process, which continues until the desired resolution is achieved. The algorithm works extremely well in the presence of noise. Tests indicate a reduction of two to eight times in processing time over conventional peak finding methods. Current implementation of the peak finding algorithm detects nuclei within liver tissue cells at Carnegie-Mellon University.

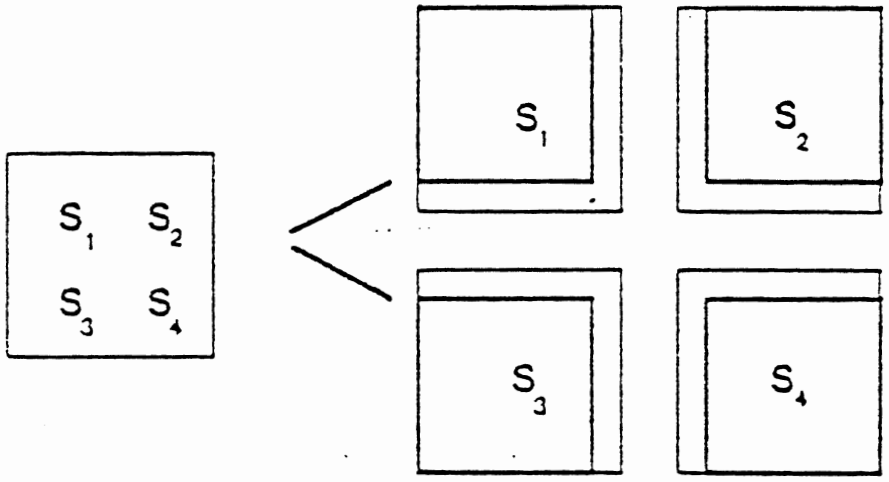

Source: O'Gorman and Sanderson (1984)

Figure 10. Detecting Gray Level Peaks

Successful segmentation of an object makes interpretation possible. One form of object interpretation is shape analysis.

Shape Recognition

Shape recognition has been a central problem in pattern recognition for many years. In particular, much attention has been focused on detecting the shape of two-dimensional planar objects. Objects have been segmented from the background and are usually represented in a binary image.

Pavlidis (1978, 1980) has provided a survey of algorithms which analyze the shape of two-dimensional binary objects. Algorithms are categorized as internal or external, and within these categories, as scalar transforms or space domain techniques. Internal algorithms use all the object points, whereas external algorithms are based only on the boundary points of an object. Pavlidis also suggests the concept of information preserving (or non-preserving) to classify shape algorithms. Information preserving algorithms have the capability of reconstructing the original shape, at least approximately, from the shape descriptors.

Internal Scalar Transforms

A procedure to represent binary patterns is discussed by Nagy (1969), with implication for use in optical character recognition. The procedure decomposes an (m X n) binary pattern into the product of a (m X k) feature matrix and a (k X n) assign-

ment matrix. Maximum coding efficiency is obtained when k is minimum. Binary matrices are generally limited to optical character recognition.

A broader approach to shape description involves the calculation of moments (Hu, 1962). Originally introduced in classical mechanics, the two-dimensional $(p+q)^{th}$ order moments of a density distribution function, p(x,y), is denoted by,

$$m_{pq} = \int_{-\infty}^{\infty} \int_{-\infty}^{\infty} x^p y^q p(x,y)\ dxdy \qquad (2\text{-}15)$$

Hu has shown that simple linear combinations of moment values yield scalar quantities which are invariant under translation and rotation. The use of "moment invariants" to describe shape was pursued by Dudani et al. (1977) to recognize different aircraft. Dudani used two different sets of seven moments; one based on internal points, the other only on the contour points. Bayes classifier and a nearest neighbor rule were used to associate moment descriptors calculated from an unknown aircraft with the descriptors of known aircraft. Results demonstrate the technique is very reliable under certain similarity transforms.

Moment calculations are information preserving, but the preservation can generally be attributed to only the first few moments. Higher-order moments are difficult to relate to shape and their implementation requires vast amounts of computer processing. Not many researchers are currently pursuing the use of moment invariants to describe shape.

Pavlidis (1978) has suggested using the two-dimensional Fourier transform on the characteristic function of an object. The characteristic function is unity for points on the object, zero elsewhere. The coefficients of the transform convey shape information. The Fourier transform is more commonly used on boundary points.

External Scalar Transforms

External scalar transforms use boundary points as input to the Fourier transform. Two approaches have been used to encode boundary points.

One approach encodes the boundary as a function of tangent angle and arc length (Zahn and Roskies, 1972; Bennet and McDonald, 1975; Chellappa and Bagdazain, 1984). Let θ_k be the angle formed between a tangent at boundary point k and a tangent to some initial point. The distance along the boundary between the initial point and point k is called the arc length, denoted by l_k. Arc length is normalized to range between 0 and 2π. The normalized function,

$$a(l_k) = \theta_k + \frac{2\pi l_k}{L} \qquad (2\text{-}16)$$

is used to encode boundary points. For a polygon, $a(l_k)$ will be linear along straight lines. Negative jumps will occur across convex angles and positive jumps across concave angles. For example, a regular polygon produces a sawtooth waveform. Figure 11 depicts the generating function of an L-shaped object.

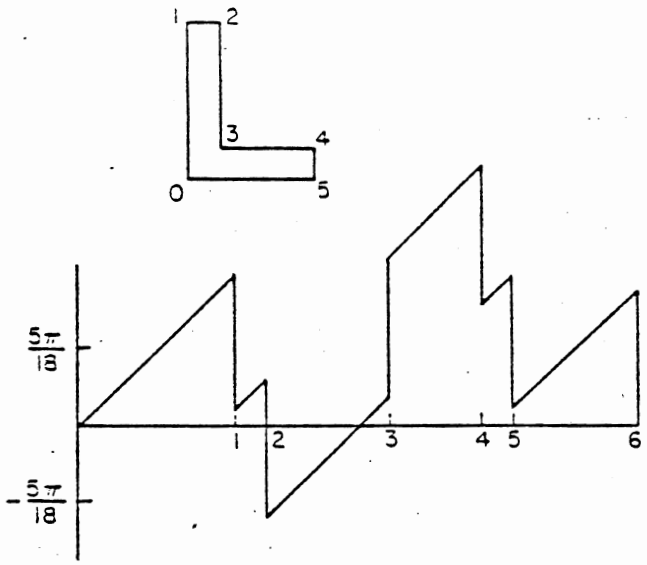

Source: Pavlidis (1978)

Figure 11. Fourier Descriptors

In general, strokes or lobes extending from the main body of an object produce peaks in $a(l_k)$ which if repeated, can be represented as coefficients in the frequency domain. Coefficients in the frequency domain are called shape descriptors. An expression to calculate the shape descriptors of the sequence $a(l_k)$ is given by,

$$S_n = \int_0^{2\pi} a(l_k)\ e^{-jnt}\ dt \qquad (2\text{-}17)$$

Interestingly, a circle produces an encoded sequence which is identically zero. The tangent angle is exactly cancelled by the normalized length function. Zahn and Roskies point out, "Viewed in this light, the function $a(l_k)$ measures the way in which the shape in question differs from a circular shape."

Correct sampling of an object's boundary is crucial to the success of Zahn and Roskies' method. A procedure to uniformly sample boundary points is discussed by Shahraray and Anderson (1985). Minimizing the number of samples and number of bits used to encode each sample is detailed by Zabelle and Koplowitz (1985).

Fourier descriptors are, in general, information preserving. However, when a subset of S_n is used to reconstruct the original boundary, the boundary does not close. Characterization of the closure property has been pursued by Strackee and Nagelkerke (1983).

An alternative method of obtaining Fourier descriptors is based on a complex sequence. The sequence, b(t), is formed from consecutive x, y coordinates along the boundary which are defined as real and imaginary components, respectively (Granlund, 1972; Persoon and Fu, 1974). The shape descriptors are calculated from,

$$T_n = \frac{1}{L}\int_0^L b(t)\ e^{-j2\pi n/L}\ dt \qquad (2\text{-}18)$$

One major difference between the method proposed by Granlund (later developed by Persoon and Fu) and the method of Zahn and Roskies is that the former produces N/2 descriptors, whereas there are N, S_n descriptors. The reduction in the number of descriptors is a direct consequence of b(t) being complex. T_n coefficients have less energy in the high frequency range than S_n coefficients. The change in spectral distribution is caused by b(t) generally being continuous, whereas $a(l_k)$ usually manifests discontinuities. T_n descriptors have the property of closure when reconstructing the original curve.

Fourier descriptors have the advantage of being backed by well-established mathematical theory. Translation, rotation, and changes in scale do not hinder the effectiveness of Fourier descriptors. Geometric stability makes the descriptors useful for recognizing handwritten numerals (Persoon and Fu, 1977).

Fourier descriptors can be implemented in real-time. Detecting pen movement has been used to automatically read hand-written characters (Arakawa et al., 1978).

Agricultural products have been examined. Fourier descriptors were used to distinguish the difference in shape between an apple and orange (Yoshio et al., 1980).

As with any transform technique, Fourier descriptors are unable to describe local information (Rice, 1969). Partially occluded objects cannot be detected. Symmetric curves can be distinguished only on the basis of phase, thus problems may occur when attempting to distinguish between a "2" and a "5".

Internal Space Domain Techniques

One simple method to detect a particular shape is template matching. Template matching performs a one-to-one comparison of each pixel between a "model" image and the image being examined (Fu, 1982b). Little or no discrepancy between images indicates the presence of a particular object. Many inspection systems for printed circuit boards use template matching (Pope, 1978; Ito, 1974). A serious limitation of template matching is the requirement of precise spatial registration between images.

Perimeter squared divided by area (p^2/A) can be used as a rough measure of shape. Bacus and Gose (1974) used p^2/A to detect a particular type of blood cell. Rosenfeld (1974b) has discussed some peculiarities when p^2/A is used to describe

certain polygons. In general, p^2/A is not information preserving.

The earliest and most widely studied internal space domain technique is the medial axis transform, originally proposed by Blum (1964). A two-dimensional planar shape is transformed into a line drawing according to the following rule. Let O be the set of points representing an object and B be the set of points representing the object's boundary. A point X, in O, is a medial axis point if it has a pair of opposing neighbors which are closer to B than X.

An analogy of the the medial axis transform has been presented by Calabi and Hartnett (1968). Assume O is uniform dry grass on bare dirt. A prairie fire begins simultaneously over B and burns inward toward the center of O. Points where fire meets fire are medial axis points. Based on this analogy, medial axis points are sometimes called quench points.

Example objects and their corresponding medial axis points are shown in Figure 12. In most instances, reconstructing an approximate boundary from the medial axis is possible, but only at the expense of intense computation (Rosenfeld and Pfaltz, 1966). Noise confounds the process of deriving the original shape. Small "dents" in an object's boundary or interior holes produce drastically altered results.

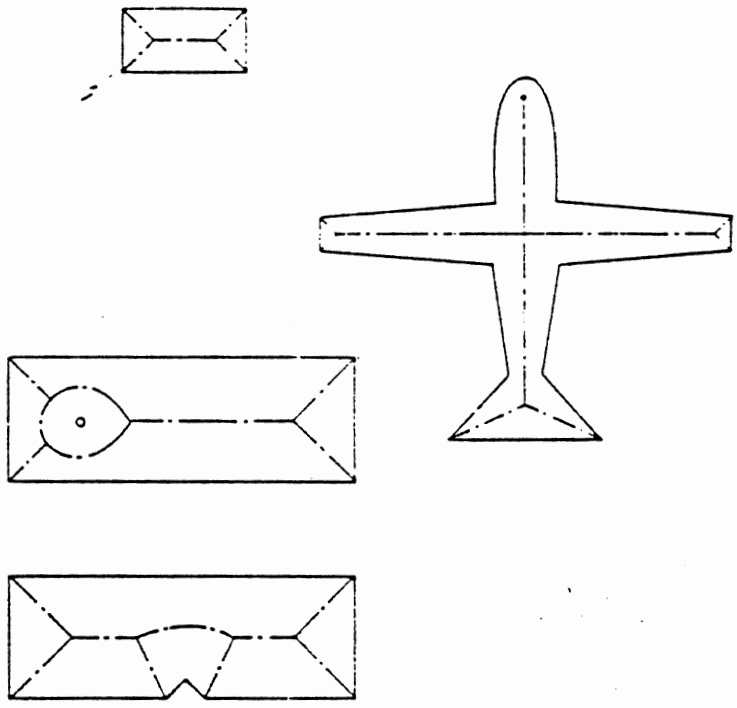

Source: Pavlidis (1978)

Figure 12. Medial Axis

Rosenfeld and Kak (1976) suggest a parallel implementation of the medial axis transform. A test to examine the neighbors of each pixel is performed simultaneously over the image. If a pixel has object pixels for all of its neighbors (a maximum of 8), then the pixel is labeled as internal. Boundary pixels will have at least one background pixel for a neighbor. An accumulator matrix is incremented for the location of each internal pixel, and boundary pixels are deleted. The test is repeated until no more object pixels are left. Local maxima in the accumulator matrix identify medial axis points.

Blum and Nagel (1977) have proposed a method similar to the medial axis transform. Their method is particularly useful when local irregularities in the boundary occur. Circles are positioned within the object so as to touch the boundary (but not cross it) in at least two points. The center of each circle is incorporated into a hierarchical data structure which can be used to reflect the object's original shape.

Wahl (1983) has introduced a distance mapping procedure based on border-to-border distance, rather than the pixel-to-border distance used by the medial axis transform. For each object point, the maximum and minimum distance to the boundary is calculated. Runlength encoding is used to calculate the distances. The minimum, maximum, and the ratio of maximum-to-minimum are used to describe shape.

Techniques related to integral geometry have been pursued. Objects are intersected by lines which form chords at various angles and positions. Statistics on the distribution of chord lengths are use to describe shape. Rutovitz (1970) used radial chords to describe the shape of chromosomes. Pavlidis (1968b) used orthogonal chords to describe the shape of typewritten characters.

Shape matrices used by Peli (1981) and Goshtasby (1985) is another interesting internal technique. Polar coordinates are used to sample an object over equally spaced angles with increasing radii (Figure 13). A binary matrix records whether or not each sample point was on the object. The rows of the matrix correspond with circles of differing radii. Columns represent equally spaced sampling points along the circumference of a circle. A silhouette formed by the transition between binary values in the shape matrix is called a shape signature. Shape signatures are one-dimensional sequences and can be correlated with other signatures to measure similarity between two objects. Shapes can also be compared by EXCLUSIVE-ORing corresponding elements of two shape matrices (Goshtasby, 1985). If the resulting matrix is sparsely populated, the two matrices are similar. Shape matrices are information preserving and invariant to translation, rotation, and scaling.

Objects can be decomposed into simple polygons to approximate shape (Frischkopf and Harmon, 1961). Pavlidis (1968a) pursued the idea by developing the concept of primary

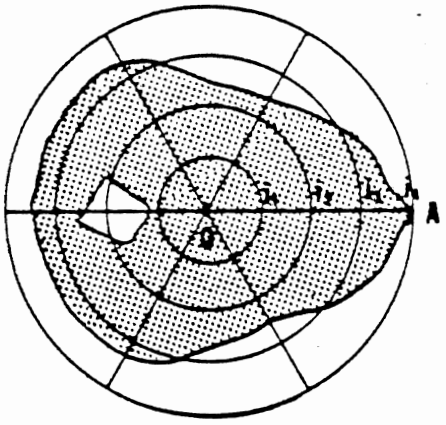

(a)

	0	1	2	3	4
0	1	1	1	1	1
1	1	1	1	0	0
2	1	1	1	1	0
3	1	1	0	1	0
4	1	1	1	1	0
5	1	1	1	0	0

(b)

Source: Goshtasby (1985)

Figure 13. Shape Matrices

convex subsets. Graphical representation of primary convex subsets has been enhanced by a relaxation labeling technique developed by Rutkowski et al. (1981). Bjorklund and Pavlidis (1981) extend some of the concepts of graphical shape recognition. Polygon approximation can also be used to remove boundary noise when using the medial axis transform (Montanari, 1969).

Recursive decomposition may offer an efficient method of shape analysis (Chaudhuri, 1985). Quadtree, octree, and binary tree data structures are used to partition the image into successively smaller regions. If a region contains an object point, it represents part of an object; otherwise, the region represents part of the background. The boundary lies between adjacent object and background regions. More accurate boundary approximations can be obtained by using smaller regions (the smallest would be a single pixel). Execution time is proportional to the number of regions.

External Space Domain Techniques

An early theory of image processing identifies curvature as one of the most important components of shape description (Attneave, 1954). Curvature is accepted by most authors as being used either explicitly or implicitly by the majority of published shape algorithms (Pavlidis, 1980b). Pavlidis defines curvature as,

> It is generally agreed that the angle between successive elementary vectors (lines joining the sample points) of a curve is a measure of the curvature, . . .

Freeman (1978a) interprets the curving of a boundary as, " ... a concatenation of arcs of varying instantaneous radii of curvature, possibly interspersed occasionally by discontinuities."

Freeman (1978a) developed the idea of critical points to describe shape. Discontinuities, endpoints, intersections, maxima, minima, and inflection points are defined as critical points on a curve. The term, 'critical', refers to the relative importance in describing the overall shape. Critical points are selected from the chain code of a curve and used to calculate five dimensionless geometric quantities. Values describe shape independently of scale, rotation, and translation. Research using critical points continues to be of interest (Yogendra and Jones, 1984; Fischler and Bolles, 1986).

Critical points are similar to a concept called multiscaling (Asada and Brady, 1986; Mokhtarian and Mackworth, 1986). The curvature of an object's boundary is analyzed to determine critical sampling points. Sampling points coincide with the zero crossings of Gaussian smoothed derivatives of boundary curves. An interesting unique property of the Gaussian filter is the assurance of no additional zero crossings for coarser filters (Yuille and Poggio, 1986; Babaud et al., 1986).

Higher-order chains can produce finer angle resolution when encoding a curve (Freeman, 1978b; Freeman and Saghri, 1978). In addition to the original 8 directions, chains have been tested for 4, 16, 24, 32, and 48 directions (Figure 14). Increased angle resolution produces a smoother approximation of

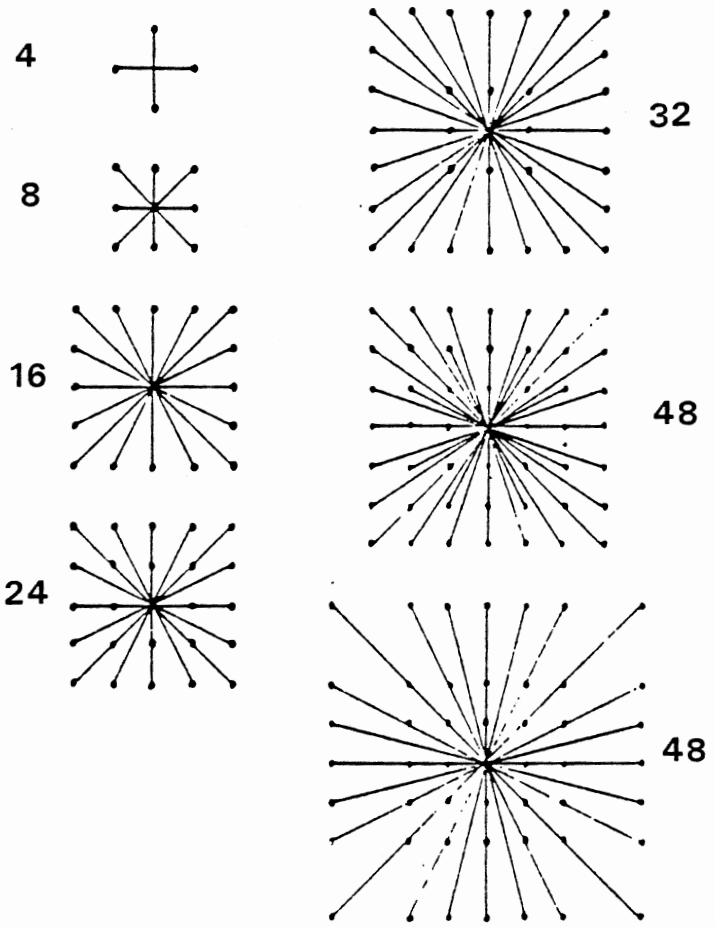

Source: Pavlidis (1980)

Figure 14. Extended Chain Codes

a curve. Also, a longer code sequence for each step reduces overall processing time. Directional codes based on 16 and 24 points were judged optimal for encoding map boundaries.

Eccles et al. (1977) used the chain code to define a curvature chain code. Curvature chain elements, s_i, are calculated from the chain code sequence, d_i, by

$$s_i = [(d_i - d_i + 11) \text{ MOD } 8] - 3 \qquad (2\text{-}19)$$

Noise in d_i will generate false indications of curvature in s_i. In order to avoid false curves, an averaging filter was used on the chain code sequence. Points in s_i were judged significant or insignificant according to their value. Shape is described by segmenting s_i into sequences bounded by significant points.

Polygon approximation of convex shapes has been based on local maxima of boundary curves (Pavlidis, 1977; Pavlidis and Horowitz, 1974). Boundary segments exhibiting a high degree of curvature are defined as corners, and corners are used to define a polygon. One difficulty in polygon approximation is that corners are more difficult to define for the discrete case than for continuous mathematics. Spline theory is useful for relating curvature maxima to corners (McClure, 1975). If the boundary contains local noise, false corners may be detected. Functional approximation may be useful to avoid detecting false corners (Rosenfeld and Johnston, 1973). A study by Davis (1977) shows that processing time for polygon approximation is propor-

tional to the square of curve length, and in some cases, to the length cubed.

Curves can be approximated by a combination of straight lines and circular arcs (Perkins, 1978). Straight lines were fit using a closed formula while the circular arcs were approximated using Newton's method. The boundary is a concatenation of straight line segments and circular arcs. Perkins suggested that the model may be useful for detecting partially occluded machine parts.

Shape description from boundary curves is particularly appropriate for syntactic pattern recognition. Boundaries are approximated by a series of segments (straight line, corner, circular arc, etc.). Segments are input into a higher level parser to describe structures (concavities, strokes, lobes). A sequence of structures can be analyzed to describe a particular shape.

The use of string grammars first occurred over thirty years ago (Chomsky, 1964). Linguistic researchers were attempting to develop a computational grammar for the purpose of automating the translation of English sentences. To date, a machine to interpret the English language has not been developed, but there have been many spin-offs of linguistic research which have benefited other disciplines. Compiler design, computer languages, automata theory, and recently, image processing and pattern recognition have made use of progress in linguistic modeling.

Gonzales and Wintz (1977) provide a simple example to illustrate some of the basic principles behind syntactic pattern recognition. The basic unit of shape description is called a primitive. A "staircase" shape is described in terms of two primitives: a horizontal vector, and a vertical vector (Figure 15). Two variables, S and A, are used to define three production rules. Production rules define variables in terms of other variables and/or primitives. The rules are,

1. S -> aA
2. A -> bS
3. A -> b

From these three production rules, an infinite number of different length "staircases" can be described. All strings begin with a special symbol called a starting symbol. In this example, the starting symbol is S. Rule 2 replaces the variable A with the concatenation of primitive b and the starting variable S. Thus, rule 2 perpetuates the sequence. Rule 3 terminates the string. The sequence of rules to define the "staircase" of Figure 15 is 121212121213.

A classical example of using a syntactic grammar is the description of submedian and telocentric chromosomes (Ledley, 1964). Ledley defines a set of primitives which consists of a series of different arcs and a straight line segment. An unknown chromosome shape can be described in terms of a set of production rules. Algorithms detect the similarity between shapes by analyzing production rules.

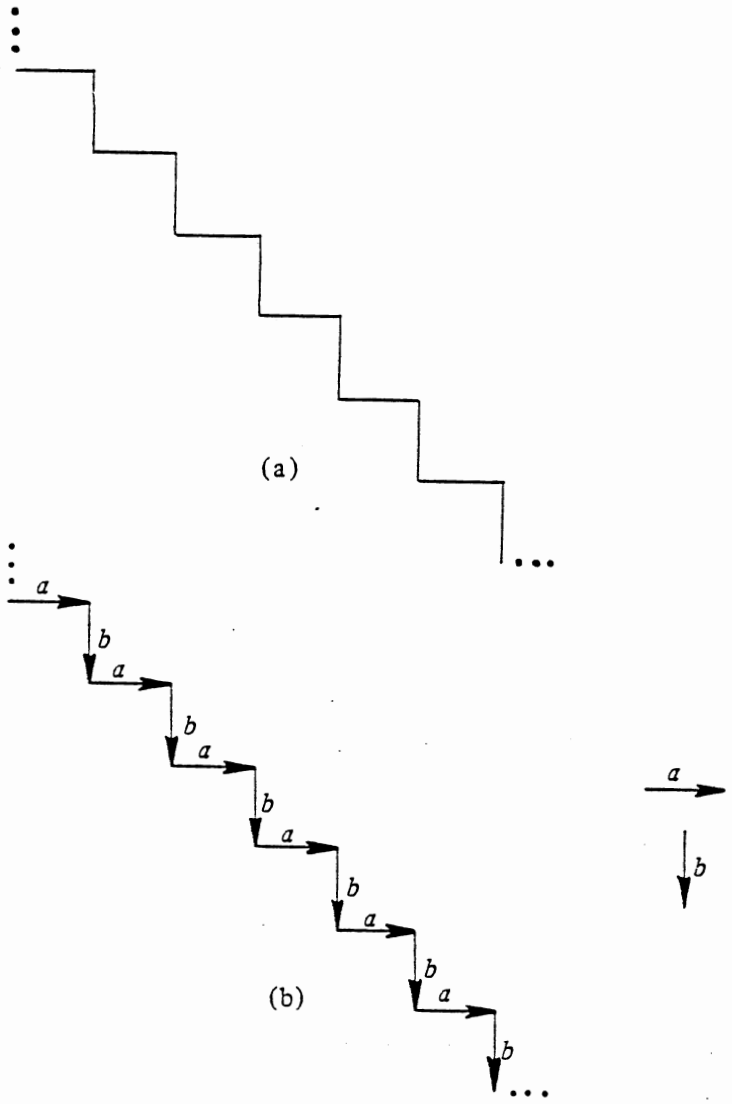

Source: Gonzales and Wintz (1977)

Figure 15. A Syntactic Descipition

Freeman's chain code is commonly used as an input to syntactic analyzers. In fact, Shaw (1970) has developed a computer language based on the chain code called Picture Description Language (PDL). The language uses four directional primitives and a negating operator to represent the eight directions of the chain code. Fu and Lu (1977) use PDL to investigate transformations which generate one string from another.

The chain code has been used in string grammars for variety of applications. Jarvis (1976) used the chain code to efficiently detect circuit board faults. Mckee and Aggarwl (1977) recognized an array of different objects. Strings representing each object are stored in a library. An algorithm detects the best match between the string of an unknown object and a stored string. String matching techniques can be enhanced by a recently introduced merge operation (Tsai and Yu, 1985). Merging shows some promise for finding matches among noisy strings.

A statistical approach to external shape description has been used by Dubois and Glanz (1986). They classify shape from an autoregression model. The same function used by Zahn and Roskies (1972) for input to the Fourier descriptors is used as input to a least squares model. The technique shows promise for recognizing a variety of industrial shapes independent of scale, translation, and rotation.

An external algorithm apart from curvature is the Hough transform (Hough, 1962). The Hough transform is not useful for general shape description, but instead, the transform is used to detect a specific shape. In fact, many algorithms that detect specific shapes are extensions of the Hough technique (Bhanu and Fuageras, 1984; Sloan, 1982; Turney et al., 1985; Algar and Thiel, 1981).

The idea behind the Hough transform may not be entirely due to Hough. Significant similarities exist between the Hough transform and a transform which is over a half century old -- the Radon transform (Deans, 1981). Radon (1917) introduced the integral,

$$F(\theta,p)=R\{F\}=\int\int_D f(x,y)\,\delta(p-x\cos\theta-y\sin\theta)\,dxdy \quad (2\text{-}20)$$

where f(x,y) represents a two-dimensional image intensity function over the planar area, D. Four important properties of the Radon transform are:

1) If f(x,y) is concentrated at a point (x_o, y_o), then F is nonzero along a sinusoidal curve $p = x_o\cos\theta + y_o\sin\theta$,

2) A point in f(x,y) corresponds to a line defined in F,

3) Collinear points in f(x,y) map to sinusoidal curves in F, all of which intersect at a point,

4) Points lying along the curve $p = x_o\cos\theta+y_o\sin\theta$ in F, correspond to lines in f(x,y) all of which intersect at x_o, y_o.

These same four properties are defined by Duda and Hart (1972) in discussing the Hough transform.

Implementation of the Hough transform involves the use of an accumulator matrix. To detect lines, the elements of the accumulator array represent every possible combination of slope and intercept (memory requirements are quite substantial). For each pixel in the image, accumulator elements which correspond to all possible slope-intercept combinations of the pixel are incremented. Lines are indicated by maxima in the accumulator matrix.

Sloan and Ballard (1980) and Ballard (1981) have extended the Hough transform to detect arbitrary shapes by the Ghough transform. In addition to an accumulator matrix, an R-table is required. The R-table records information which describes the relative position of each boundary pixel with respect to some reference point. To detect an unknown object, possible center locations are calculated from the object's boundary points according to the rules in the R-table. For each possible center location, an element in accumulator array is incremented. By including rotation and scaling factors in the R-table, geometric invariance is achieved.

The Hough transform is particularly suited for detecting occluded objects (Whittaker et al., 1984; Turney et al., 1985). Each point "votes" independently for a particular overall situation. If points tend to follow some spatial relationship,

parameters defining that relationship can generally be detected.

Brown (1983) has investigated a method to obtain a more noise-free estimate of shape parameters. The Chough (complimentary Hough) transform attempts to recognize the presence of unlikely parameter-space combinations and negate these values. Thus, more distinct maxima are present in the accumulator array.

Memory and processing requirements create a severe limitation to Hough-related techniques. Resource requirements increase exponentially as the number of parameters increase. Many current approaches are attempting to alleviate large computational requirements by incorporating an updated "best guess" estimate (Turney et al., 1985). Kimme et al. (1975) used gradient direction to assist in locating circular tumors from an edge-enhanced chest X-ray image.

The Fourier Transform

An image transform which appears frequently in the literature of image processing is the Fourier transform (Titchmarsh, 1948). The Fourier transform of a two-dimensional function, f(x,y), is described by,

$$F(u,v) = \int_{\infty} \int f(x,y)\ e^{-j2\pi(ux+vy)}\ dxdy \qquad (2\text{-}21)$$

where u and v are frequency variables. From Euler's formula, the exponential term can be approximated by,

$$e^{-j2\pi(ux+vy)} = \cos(2\pi(ux+vy)) - j\sin(2\pi(ux+vy)) \quad (2\text{-}22)$$

Thus, F(u,v) can be regarded as describing how f(x,y) changes in terms of sinusoidal ocillations.

F(u,v) is generally complex, consisting of a real part, R(u,v), and an imaginary part, I(u,v). Some commonly used quantities to describe the distribution of F(u,v) are the magnitude and phase. The magnitude of F(u,v) is defined by,

$$|F(u,v)| = \sqrt{R(u,v)^2+I(u,v)^2} \quad (2\text{-}23)$$

and the phase by,

$$\phi(u,v) = \mathrm{Tan}^{-1}\left[\frac{I(u,v)}{R(u,v)}\right] \quad (2\text{-}24)$$

The energy spectrum of F(u) is represented as E(u) and is the square of the magnitude of F(u).

Fourier-Bessel Transform

Lenses inherently produce a small amount of spherical aberation. This type of distortion can be approximated by a circularly symmetric function. Therefore, it is convienient to describe f(x,y) in terms of polar coordinates, $f(r,\theta)$. The coordinate transformation from a rectangular to a polar coordinate system is accomplished by,

$$\begin{aligned} r &= \sqrt{x^2+y^2} \quad & x &= r\cos\theta \\ \theta &= \tan^{-1}\left[\frac{y}{x}\right] \quad & y &= r\sin\theta \end{aligned} \quad (2\text{-}25)$$

The frequency variables are related by,

$$\rho = \sqrt{u^2+v^2} \qquad u=\rho\cos\phi$$
$$\phi=\tan^{-1}\left(\frac{u}{v}\right) \qquad v=\rho\sin\phi \tag{2-26}$$

The Fourier transform in polar coordinates is accomplished by making the appropriate substitutions into equation 2-21,

$$F(\rho,\phi) = \int_0^{2\pi}\int_0^{\infty} f(r,\theta)\, e^{-j2\pi r\rho(\cos\theta\cos\phi+\sin\theta\sin\phi)}\, r\,dr\,d\theta \tag{2-27}$$

Note the incremental area, dxdy, equates to $rdrd\theta$ in polar coordinates. Exchanging the order of integration and simplifying,

$$F(\rho,\phi) = \int_0^{\infty}\int_0^{2\pi} rf(r,\theta)\; e^{-j2\pi r\rho\cos(\theta-\phi)}\; d\theta\,dr \tag{2-28}$$

Since the spherical aberation is circularly symmetric,

$$f(r) = f(r,\theta) \tag{2-29}$$

This simplifies equation 2-28 to,

$$F(\rho) = \int_0^{\infty} rf(r)\int_0^{2\pi} e^{-j2\pi r\rho\cos\theta}\, d\theta\,dr \tag{2-30}$$

since rf(r) is no longer a function of θ. By definition, the inner-most intergral is equivalent to,

$$2\pi J_0(2\pi r\rho)$$

where J_0 is a Bessel function of the first kind, zero order. For a circularly symmetric function, the Fourier transform in polar coordinates is described by,

$$F(\rho) = 2\pi \int_0^{\infty} rf(r)\ J_0(2\pi r\rho)\ dr \qquad (2\text{-}31)$$

Equation 2-31 is called the Fourier-Bessel transform, or alternatively, the Hankel transform of zero order. The Hankel transform ocurrs frequently in the optical signal processing literature. (Stark, 1982; Goodman, 1968).

CHAPTER III

METHOD AND PROCEDURE

Introduction

To enable a vision system to recognize an object in a digital image, pertinent image features of the object must first be identified. Usually, the features will obey some rule according to the object's geometry. Writing an accurate mathematical description of these rules provides a basis for an object recognition algorithm.

In most instances, objects will have more than one pertinent feature, and for each feature, more than one mathematical description. Unfortunately, the relative importance of each feature and accuracy of the mathematical description are not always apparent. Often, the problems of a particular approach are discovered only after the approach has been implemented.

Chapter three describes four attempts to develop an algorithm to recognize pine seedlings. These attempts are:

1. gray level peaks,
2. geometric line intersections,
3. gray level contours,
4. A Fourier transform technique.

Gray Level Peaks

When an image is formed from an overhead view of a seedling bed, it is possible to increase the field of view so that individual seedlings approximate small circular regions. Increasing the field of view effectively reduces the spatial sampling rate, which in turn precludes accurate representation of the pine needles. This seemingly undesirable result can be used to advantage because it creates a one-to-one correspondence between seedlings and gray level peaks.

Pixels in a N x M image can be classified as gray level peaks by the operation,

$$b(x,y) = \prod_{n=0}^{7} P\{ f(x,y)-f(x_n,y_n)+1 \} \qquad (3\text{-}1)$$

for x=0, 1, 2, ... N-1 and y=0, 1, 2, ... M-1. The operator, P{}, is defined as,

$$P\{x\} = \begin{cases} x, & x>0 \\ 0, & \text{otherwise} \end{cases} \qquad (3\text{-}2)$$

The function, $f(x_n,y_n)$, represents the n^{th} neighbor of f(x,y) as depicted in Figure 6.

An image system capable of parallel convolution can implement equation 3-1 by performing a two-dimensional convolution to determine each quantity, $\{f(x,y)-f(x_n,y_n)+1\}$. This technique assumes the system automatically reset negative values to zero (as indicated by the P{} operator). Peak points are non-zero values in **B**.

If all gray level peaks produced a single isolated pixel, then the number of seedlings would be indicated by the number of non-zero pixels in **B**. However, in some instances, individual seedlings generate a peak region consisting of two or more adjacent pixels of equal value. This condition is provided for by the addition of 1 in equation 3-1. When a peak region occurs, it is necessary to include an additional processing step. A recursive algorithm to identify individual connected regions is,

```
connect(x,y)
    b(x,y) = 0;

    For n = 0 to 7 do;

        if b(xn,yn) > 0 then do;
            b(xn,yn) = 0;
            connect(xn,yn);
```

The algorithm will return to the calling routine only after all non-zero pixels connected to (x,y) have been set to zero. Individual pine seedlings can be counted by scanning over **B** and invoking the connect routine whenever a non-zero pixel is encountered. The number of seedlings will be indicated by the number of times connect is called.

In practice, it is useful to low-pass filter the image before implementing equation 3-1. Filtering helps to reduce the occurrence of peaks in the background which do not correspond to a seedling. Assuming adequate contrast, false peaks can also be avoided by global thresholding. Peak points corresponding to pixels below the threshold level are ignored.

Geometric Line Intersections

In general, pine needles can be approximated by straight lines. The geometric intersection of lines formed by pine needles should isolate the center of individual seedlings.

If the needles form lines of unit width, an N x M image, **B**, is filtered according to,

$$b(x,y) = \sum_{n=0}^{3} P\{f(x,y)-f(x_n,y_n)\}\ P\{f(x,y)-f(x_{n+4},y_{n+4})\} \qquad (3\text{-}3)$$

for x=0, 1, 2, ... N-1 and y=0, 1, 2, ... M-1. The subscripts have the same meaning as in equation 3-1. Equation 3-3 can be implemented with two convolutions and one frame multiplication for each n. Lines in **B** are found by examining the distribution of non-zero pixels. A line is defined as a chain-code sequence which obeys the rules of a straight line beyond some arbitrary length.

Examining all possible chain-code combinations can be accomplished, in part, through a parallel convolution. **B** is redefined by,

$$b(x,y) = \begin{cases} 1, & b(x,y) > 0 \\ 0, & \text{otherwise} \end{cases} \qquad (3\text{-}4)$$

Detecting the presence of pixels in **B** having non-zero neighbors can regarded as the convolution,

$$b(x,y) = b(x,y) * g(x,y) \qquad (3\text{-}5)$$

where,

$$b(x,y)*g(x,y) = \sum_{m=0}^{M-1} \sum_{n=0}^{N-1} b(m,n)g(x-m,y-n) \qquad (3\text{-}6)$$

The matrix, **G**, is defined by,

$$\begin{bmatrix} 2^0 & 2^1 & 2^2 \\ 2^3 & 0 & 2^4 \\ 2^5 & 2^6 & 2^7 \end{bmatrix}$$

Elements outside the 3 x 3 range of **G** are zero. This procedure assumes **B** has a gray scale resolution of eight bits. After applying equation (3-5), values in **B** encode the distribution of pixels in the original image.

Lines are detected by masking pixels in **B** by value. For example, vertical lines could be isolated by,

$$b(x,y) = \begin{cases} 1, & b(x,y) = 2,\ 32,\ 34 \\ 0, & \text{otherwise} \end{cases} \qquad (3\text{-}7)$$

Repeated applications of equations 3-5 and 3-7 can be used to threshold lines on the basis of length. Pixels not connected according to equation 3-7 will vanish within the first few iterations. After n iterations, non-zero values in **B** will gaurantee the existence of a line at least 2n pixels in length.

In practice, lines formed by the needles rarely coincide at a single geometric center. Because of this problem, the intersection was defined as the (x,y) coordinate which minimized,

$$c(x,y) = \sum_{l=0}^{L-1} \left| \frac{p_l x + q_l y + r_l}{\sqrt{p_l^2 + q_l^2}} \right| \qquad (3\text{-}8)$$

Equation 3-8 sums the normal distance from (x,y) to each line, where L is the total number of lines of the form,

$$px + qy + r = 0 \qquad (3\text{-}9)$$

The summation over all lines produces erratic results because the procedure does not associate the needles with any one seedling. Therefore, it is necessary to restrict the use of equation 3-8 to only those line segments within some specified distance of (x,y). The center of individual pine seedlings can then be identified by minimum values in C.

Contour Encoding

An approach which exploits changes in gray level and pine needle geometry is gray level contour encoding. The algorithm is used to outline regions of uniform gray level. A sequence of pixels is generated so that adjacent pixels external to the enclosed region will always have a different value. This condition can be achieved by employing the well-known "left-most-looking" rule. If neighbors of a pixel, f_c, are defined as,

$$\begin{array}{ccc} & f_3 & \\ f_2 & f_c & f_0 \\ & f_1 & \end{array}$$

The algorithm will attempt to move to a neighbor of equal value with preference for a relative left direction. For a reference direction of 3, the preferential sequence would follow 2, 3, 0, and 1. A recursive algorithm to implement gray level contour encoding is,

```
LML( x, y, d )
   i = 3;
   found = false;

      while( (found=false) and (i<7) )
         n = (d+i) modulo 4;

         if f(x,y) = f(x_n, y_n) then
            found = true;
            LML( x_n, y_n, n);
         else i = i + 1;
```

The coordinates of a pixel on the contour are (x,y) and d is the reference direction. Each call to LML will visit, in sequence, a single pixel on the gray level contour.

By selecting an appropriate gray level, the influence of individual pine needles on a contour can be recognized. If q_i represents the coordinate pair (x_i,y_i), the pixels on a contour can be denoted by the sequence,

$$q_0,\ q_1,\ q_2,\ \cdots,\ q_r$$

The boundary along an individual pine needle can be identified by a subsequence of length k+1 as,

$$q_s,\ q_{s+1},\ \cdots,\ q_{s+\frac{k}{2}-1},\ q_{s+\frac{k}{2}},\ q_{s+\frac{k}{2}+1},\ \cdots,\ q_{s+k-1},\ q_{s+k}$$

where s is an arbitrary starting value. Detecting an individual

subsequence can be achieved by exploiting the symmetry about $q_{s+\frac{k}{2}}$. The distance between coordinate values,

$$q_{s+\frac{k}{2}-i}, \quad q_{s+\frac{k}{2}+i}$$

remains relatively constant for $i = 0, 1, \ldots, \frac{k}{2}$.

A Fourier Transform Technique

The distribution of pixel values in a circular region centered over a pine seedling can be conveniently described in polar coordinates. Assuming the pine needles have some fixed average length, a seedling can be represented as a function of angle alone so that,

$$f(\theta) = f(r,\theta) \tag{3-10}$$

This equivalence occurs when the origin of the coordinate system coincides with the center of a seedling. The frequency content of $f(r,\theta)$ provides a quantitative measure of the validity of equation 3-10, and thus may be useful to detect individual seedlings. Unfortunately, the Fourier-Bessel transform is quite complex for the assumption of equation 3-10. The frequency content of the general function, $f(\theta)$, is described by the infinite sum,

$$F(\phi) = \sum_{k=(-\infty)}^{\infty} c_k(-j)^k \, e^{jk\phi} \, \mathcal{H}_k\{f(r)\} \tag{3-11}$$

where,

$$c_k = \frac{1}{2\pi}\int_0^{2\pi} f(\theta)\ e^{-jk\theta}\, d\theta \qquad (3\text{-}12)$$

and $\mathcal{H}_i\{\}$ represents an i^{th} order Hankel transform (Goodman, 1978).

A more direct approach to quantify the frequency content of $f(r,\theta)$ is to form a one-dimensional sequence, X, from the two-dimensional sequence, $f(r,\theta)$. This process can be described by,

$$\begin{aligned} X = {} & f(r_0,\theta_0),\ f(r_0,\theta_1),\ \ldots,\ f(r_0,\theta_{P-1}), \\ & f(r_1,\theta_0),\ f(r_1,\theta_1),\ \ldots,\ f(r_1,\theta_{P-1}), \\ & \ldots, \\ & f(r_{Q-1},\theta_0),\ f(r_{Q-1},\theta_1),\ \ldots,\ f(r_{Q-1},\theta_{P-1}) \end{aligned} \qquad (3\text{-}13)$$

where,

$$r_i = r + i\,\Delta r \quad \text{for } i = 0,\ 1,\ 2,\ \ldots,\ Q\text{-}1 \qquad (3\text{-}14)$$

and,

$$\theta_j = j\,\Delta\theta \quad \text{for } j = 0,\ 1,\ 2,\ \ldots,\ P\text{-}1 \qquad (3\text{-}15)$$

The angular increment and number of angles are chosen so that,

$$P\,\Delta\theta = 2\pi \qquad (3\text{-}16)$$

If $f(r,\theta)$ is radially symmetric, then for any value, j,

$$f(r_o,\theta_j) = f(r_m,\theta_j);\ m = 1,\ 2,\ \ldots,\ Q\text{-}1 \qquad (3\text{-}17)$$

X will be periodic with Q periods, each consisting of P points. X becomes,

$$X = x_0,\ x_1,\ \ldots,\ x_{P-1}\ ,\ \ldots,\ x_0,\ x_1,\ \ldots,\ x_{P-1} \qquad (3\text{-}18)$$

Within X, each subsequence,

$$x_0,\ x_1,\ \ldots,\ x_{P-1}$$

can be completely described by a sum of periodic components where

the number of periods in each component is an integer multiple of Q.

This result can be shown intuitively be referring back to equation 3-17. If a sequence, X', were to be periodic with K cycles, where K is not an integer multiple of Q, then the condition of equation 3-17 does not hold true since it is possible to show,

$$\begin{aligned} f(r_0,\theta_0) &= x_0 \\ f(r_1,\theta_0) &= x'_{Q \text{ MOD } K} \end{aligned} \tag{3-19}$$

Therefore,

$$f(r_0,\theta_0) \neq f(r_1,\theta_0) \tag{3-20}$$

since by definition, Q modulo K is not equal to zero when K is not an even multiple of Q.

The constraints imposed on X by radial symmetry can be shown by calculating the discrete Fourier Transform (DFT) of X. The DFT of X is defined by,

$$f_u = \frac{1}{PQ} \sum_{n=0}^{PQ-1} x_n \, e^{-j2\pi un/PQ} \tag{3-21}$$

for u = 0, 1, 2, ..., PQ-1. The first half of F represents the sinusoids of

$$0,\ 1,\ 2,\ \ldots,\ \frac{PQ}{2} - 1$$

periods per sequence, respectively.

From the previous discussion, radial symmetry implies that the non-zero coefficients in F are only those coefficients which are not an integer multiple of Q. This assumption reduces F to,

$$F = f_0,\ f_Q,\ f_{2Q},\ f_{3Q},\ \ldots,\ f_{(P-1)Q} \tag{3-22}$$

Equation 3-21 becomes,

$$f_u = \frac{1}{PQ} \sum_{n=0}^{PQ-1} x_n\ e^{-j2\pi un/P} \tag{3-23}$$

for u=0, 1, 2, ..., P-1. Representing X in terms of the Fourier coefficients in equation 3-23 yields,

$$x_i' = \sum_{u=0}^{P-1} f_u\ e^{j2\pi ui/P} \tag{3-24}$$

for i=0, 1, 2, ..., PQ-1. Substituting equation 3-23 into equation 3-24 yields,

$$x_i' = \sum_{u=0}^{P-1} \left[\frac{1}{PQ} \sum_{n=0}^{PQ-1} x_n\ e^{-j2\pi un/P} \right] e^{j2\pi ui/P} \tag{3-25}$$

for i=0, 1, 2, ..., PQ-1. Exchanging the order of summation and simplifying,

$$x_i' = \sum_{n=0}^{PQ-1} \frac{x_n}{PQ} \sum_{u=0}^{P-1} e^{-j2\pi u(n-i)/P} \tag{3-26}$$

for i=0, 1, 2, ..., PQ-1. Equation 3-26 is in a form which

readily reveals the condition of radial symmetry as defined in equation 3-17.

The value, $\frac{2\pi u}{P}$, for u=0, 1, 2, ..., P-1, generates P evenly spaced partitions over the range 0-2π. Using Euler's formula (equation 2-19), the summation of the exponential term in equation 3-26 equates to zero except for particular values of (n-i). An exception occurs when (n-i) is an even multiple of P, or when,

$$(n-i) \text{ MOD } P = 0 \tag{3-27}$$

When n and i satisfy equation 3-27, the exponential term in equation 3-26 will evaluate to unity for each value of the summation. Thus, equation 3-26 reduces to,

$$x_i' = \sum_{n=0}^{PQ-1} \frac{x_n}{PQ} \sum_{u=0}^{P-1} \phi_i(n) \tag{3-28}$$

where,

$$\phi_i(n) = \begin{cases} 1, & (n-i) \text{ MOD } P=0 \\ 0, & \text{otherwise} \end{cases} \tag{3-29}$$

for i=0, 1, 2, ..., PQ-1. Simplifying equation 3-28,

$$x_i' = \sum_{n=0}^{PQ-1} \frac{x_n}{Q} \phi_i(n) \tag{3-30}$$

for i=0, 1, 2, ..., PQ-1. For a function that is radially symmetric, the Fourier expansion of equation 3-24 is equivalent to transforming X with the basis functions, $\phi_i(n)$. The basis

functions can be interpreted as P equally spaced radial lines over 2π which extend from r to r + (Q-1)Δr.

Equation 3-30 indicates that $X = X'$ only when X is radially symmetric. For example, using equation 3-30 to evaluate x_0',

$$x_0' = \frac{1}{Q}[\, x_0 + x_P + x_{2P} + x_{3P} + \ldots + x_{(Q-1)P}] \qquad (3\text{-}31)$$

The subsequent value at the same angle is,

$$x_P' = \frac{1}{Q}[\, x_0 + x_P + x_{2P} + x_{3P} + \ldots + x_{(Q-1)P}] \qquad (3\text{-}32)$$

It is possible to show that, in general,

$$x_0 = x_{mP} \qquad (3\text{-}33)$$

for m=1, 2, 3, ..., Q-1. This result is in direct correspondence with the definition of radial symmetry in equation 3-17.

The degree to which X' approximates a radial symmetric function can be used to detect when X was sampled about the center of a seedling. Figure 16 shows two sequences, one obtained about the center of a seedling, and one sampled about an origin ten pixels off center. For each sequence, the radial symmetric approximation, as calculated by equation 3-30, is also shown. In a qualitative sense, the approximation of the on-center sequence is a relatively accurate representation of the original. The approximation of the off-center sequence is a poor representation of the original.

A common technique to measure the degree of approximation is the mean squared error,

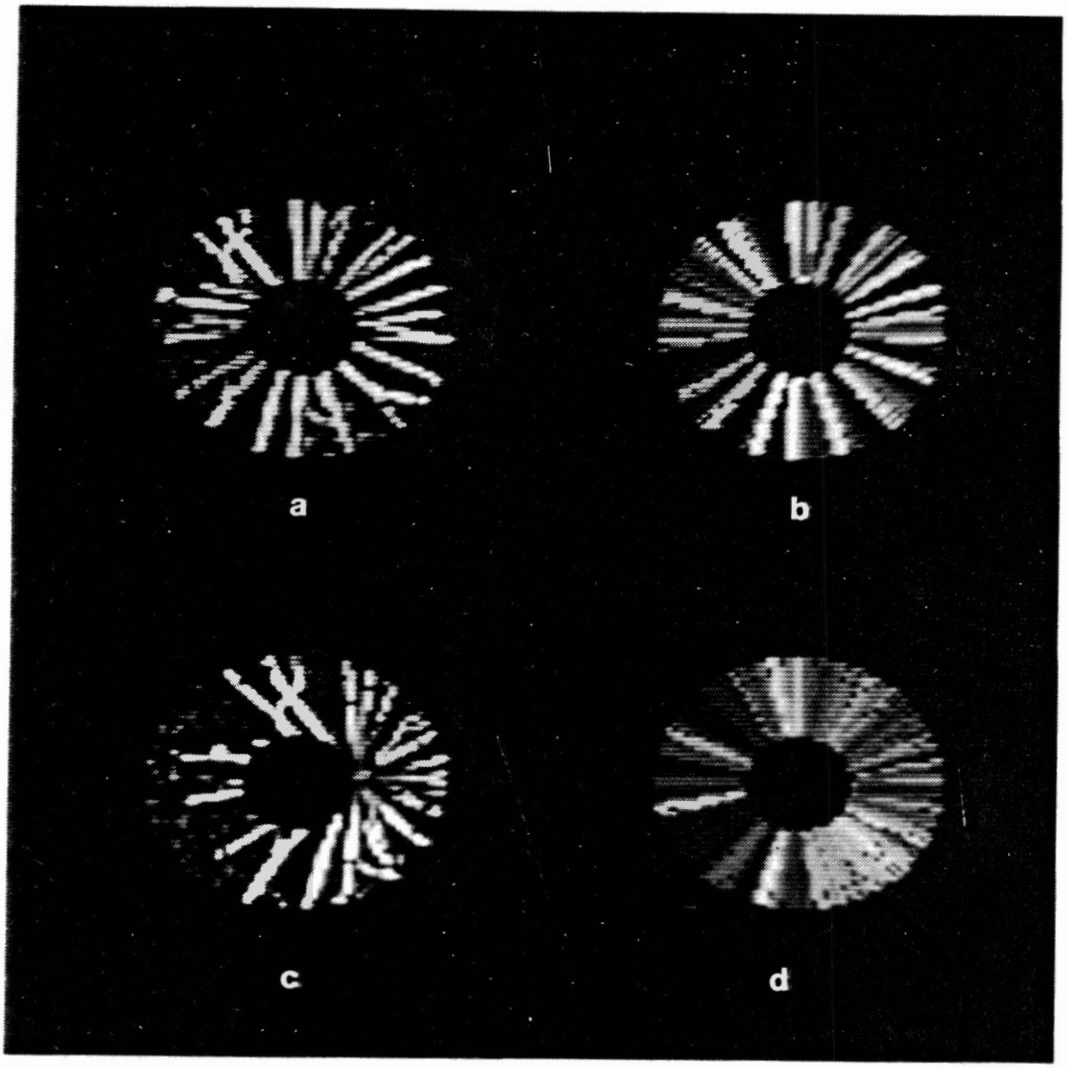

Figure 16. Radial Symmetric Approximation. (a) original on-center sequence. (b) radially symmetric approximation of (a). (c) original off-center sequence. (d) radially symmetric approximation of (c).

$$\overline{\epsilon^2} = \frac{1}{PQ} \sum_{n=0}^{PQ-1} (x_n - x_n')^2 \qquad (3\text{-}34)$$

Small $\overline{\epsilon^2}$ values result when the origin of X corresponds to the center of a pine seedling. However, the mean squared error by itself is not unique to pine seedlings. X would be radially symmetric if the sampled region were to have a uniform gray level. To avoid this ambiguity, the mean of X is incorporated into equation 3-35. A signal-to-noise ratio defined by,

$$SNR = \frac{\sum_{n=0}^{PQ-1} (x_n')^2}{\sum_{n=0}^{PQ-1} (x_n - x_n')^2} \qquad (3\text{-}35)$$

is used to isolate the center of individual seedlings.

In the absence of noise, SNR is successful at distinguishing the center of a pine seedling. Figure 17 shows three curves which plot SNR as a function of distance to the center of a pine seedling. The curve identified with a zero shows the SNR calculated directly from a relatively noise-free portion of a sample image. As distance increases, the SNR drops rapidly providing good differentiation between on-center and 10 pixels away from center.

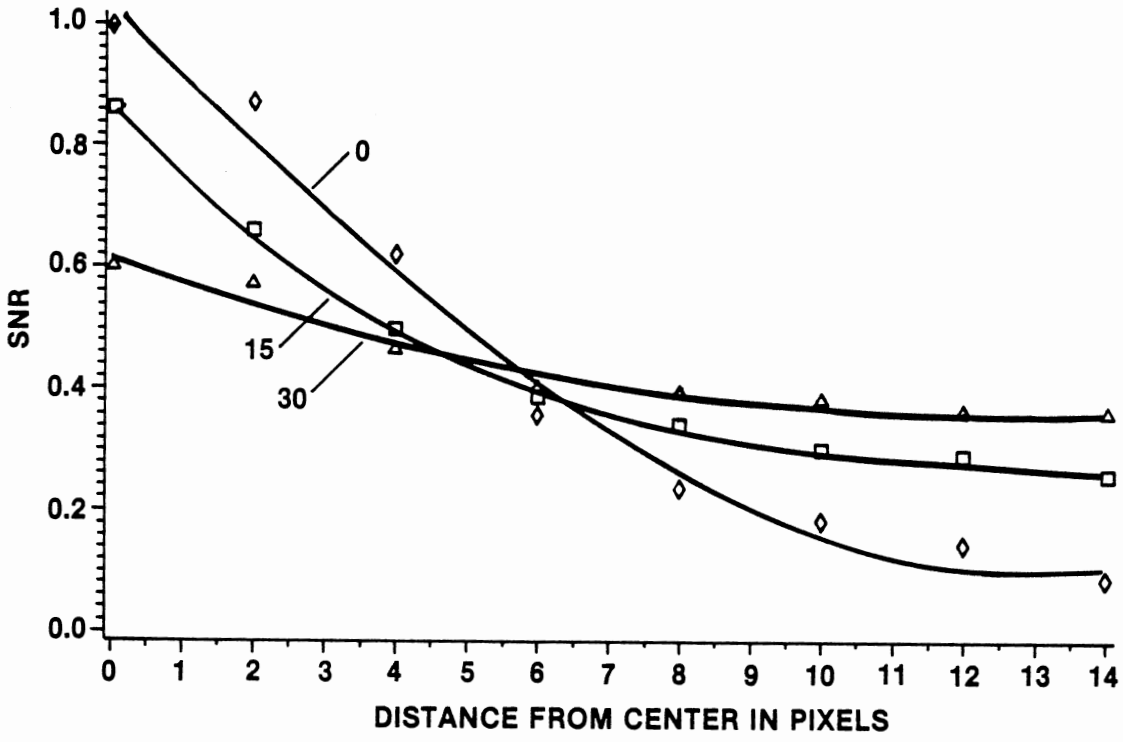

Figure 17. Signal-to-Noise Ratio to Detect Seedling Center

The performance of SNR degrades rapidly with the introduction of artificially added noise. The curve identified with a 15 in Figure 17 shows the SNR-distance relationship for the same image with the addition of noise selected at random over the range 0-15 (the image is corrupted with white noise rather than Gaussian noise). The total possible range of the input sequence is 0-255. In a similar manner, the curve identified with a 30 shows the effects of noise over the range 0-30. As the noise level increases, the capability of SNR to distinguish the center of a seedling diminishes. The degradation is primarily a result of the SNR's dependence on the mean.

As an alternative to using a SNR value, it is possible to directly exploit the energy spectrum of X. Figure 18 shows the energy spectrum, as calculated by equation 3-23, for a sequence obtained by sampling about the center of a typical seedling (the spectrum has not been centered, so coefficients from 1025-2048 represent negative frequencies shifted by 2048. This fact is apparent in the symmetry of the spectral values about coefficient 1024.)

The physiology of a pine seedling suggests a particular measurement on the energy spectrum. The primary function of the needles is to absorb energy (sunlight) and other nutrients. A seedling with even angular spacing between needles will minimize intra-needle competition and maximize energy absorption. These seedlings are more likely to survive. As a result, there is a good chance that more than one pair of needles will be sepa-

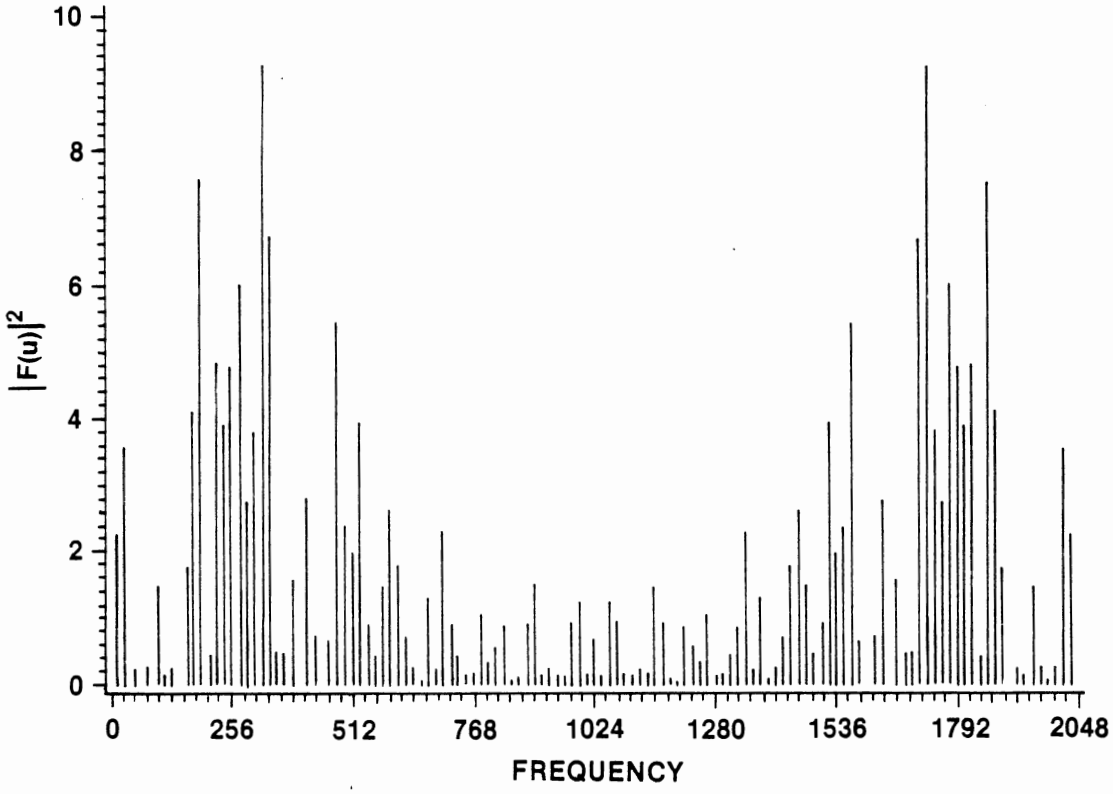

Figure 18. An On-Center Energy Spectrum

rated by the same angular spacing. If needles occur at fixed angular spacing, the energy in the spectrum will be concentrated into a single coefficient whose value would reflect the total number of needles.

To exploit this phenomenon, a maximum value from the energy spectrum is used to detect individual seedlings. A transformation is defined by,

$$g(x,y) = \sum_{x=0}^{M-1} \sum_{x=0}^{N-1} \text{MAX}\left[\sum_{n=0}^{PQ-1} x_n \, e^{-j2\pi un/P} \right] \qquad (3\text{-}36)$$

for u=0, 1, 2, ... P-1. When (x,y) coincides with the center of a pine seedling, g(x,y) will contain a local maximum. If (x,y) is slightly off-center, g(x,y) will be much smaller. Figure 19 shows the energy spectrum obtained from the same sequence shown in Figure 18, except the centroid of the sampling area is 10 pixels off-center. The maximum coefficient in Figure 19 is about half of the maximum coefficient in Figure 18.

An example image and its corresponding transform are shown in Figures 20 and 21, respectively. The blurred appearance of the transformed image is a result of only processing every fourth pixel, and interpolating to restore the original dimension. Indentifying local maxima provides a method of detecting individual pine seedlings.

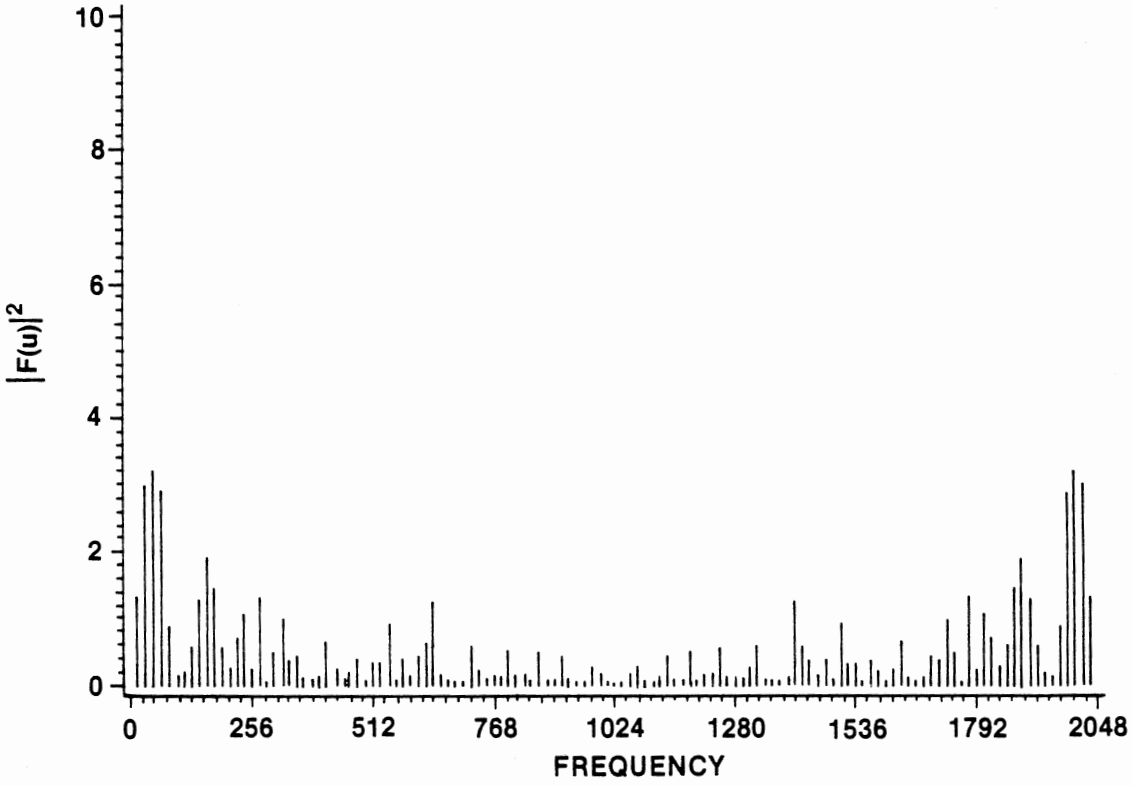

Figure 19. An Off-Center Energy Spectrum

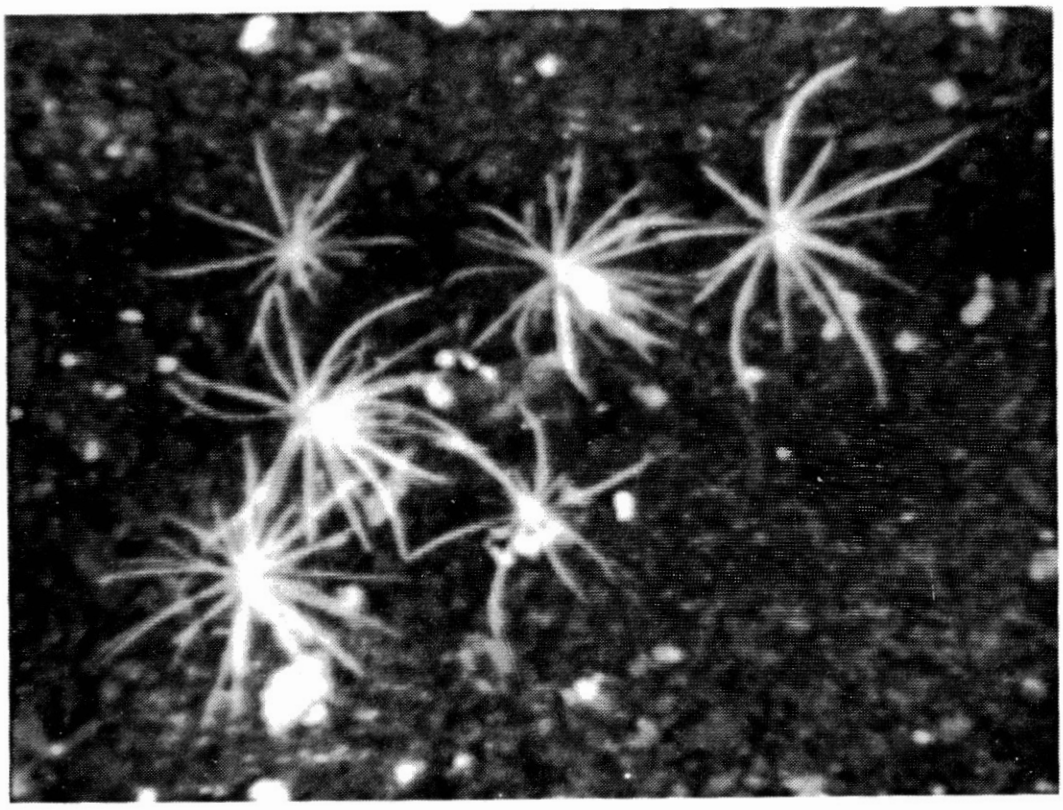

Figure 20. A Seedling Image

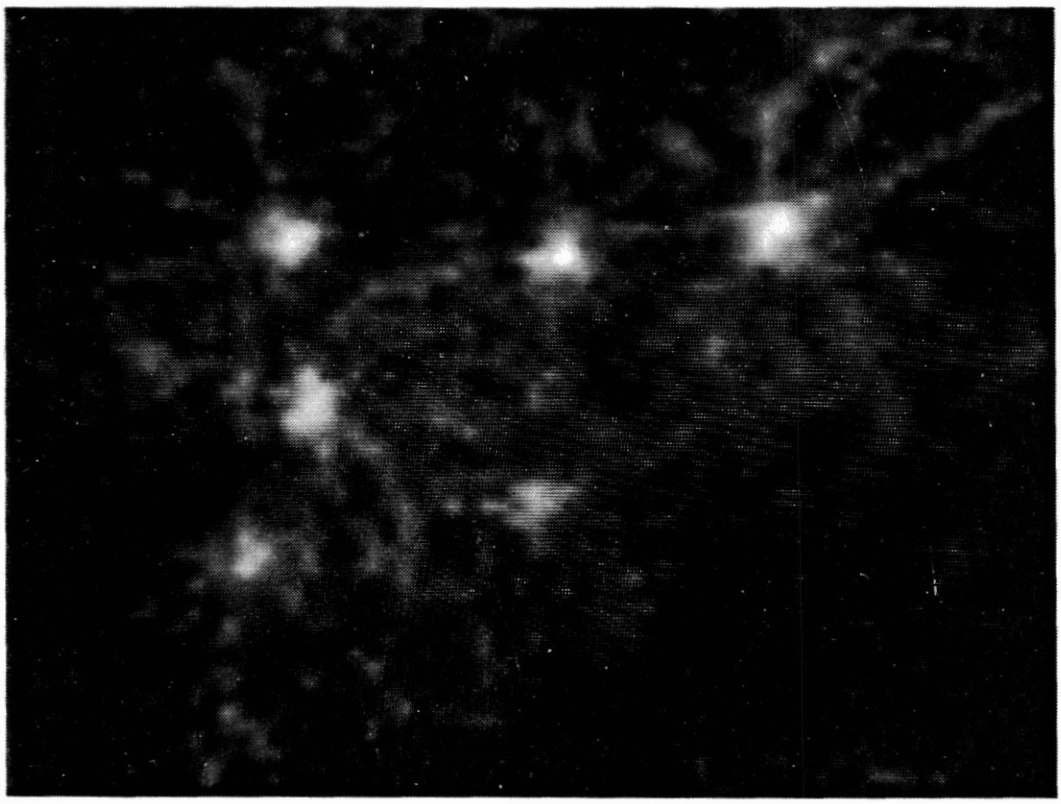

Figure 21. A Transformed Seedling Image

Equation 3-36 is relatively unaffected by noise. Figure 22 is similar to Figure 17 except that a maximum energy value, as calculated by equation 3-36, is used instead of SNR. The distinction between an on-center sequence and a sequence 10 pixels away from center is relatively unaffected by the additive noise. The noise tolerance is due, in part, to the fact that the frequency coefficients are independent of the mean of X.

Implementation

The computer system used in this investigation is a D256 development station, manufactured by International Robomation/ Intelligence (IRI, 1985). The system is designed to handle 256 x 256 image matrices, with 8 bit gray scale resolution. The camera is an Hitachi KP-120U, which uses a charged-coupled device. The necessary support hardware/software to acquire an image and manipulate individual pixels is provided with the system.

With the particular lens configuration, the pine needles cover an annular region from a radius of about 10 to 25. Therefore, Q is 16. The number of angles, P, is 128. The total length of the input sequence is 2048. The limits of the angular region, and the number of angles are beyond the resolution of the image matrix. The number of unique pixels along the circumference of different diameter circles is shown in Figure 23. The horizontal line indicates the required resolution for P=128. The angular resolution at a diameter of 11 is roughly half the

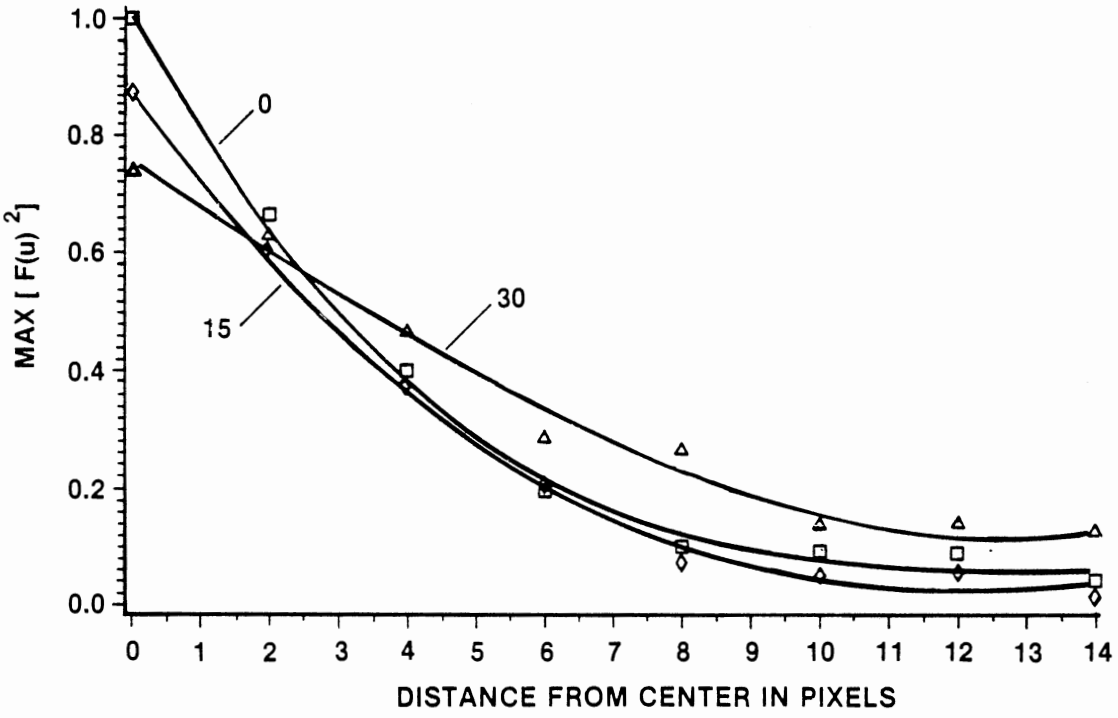

Figure 22. Maximum Energy Coefficient to Detect Seedling Center.

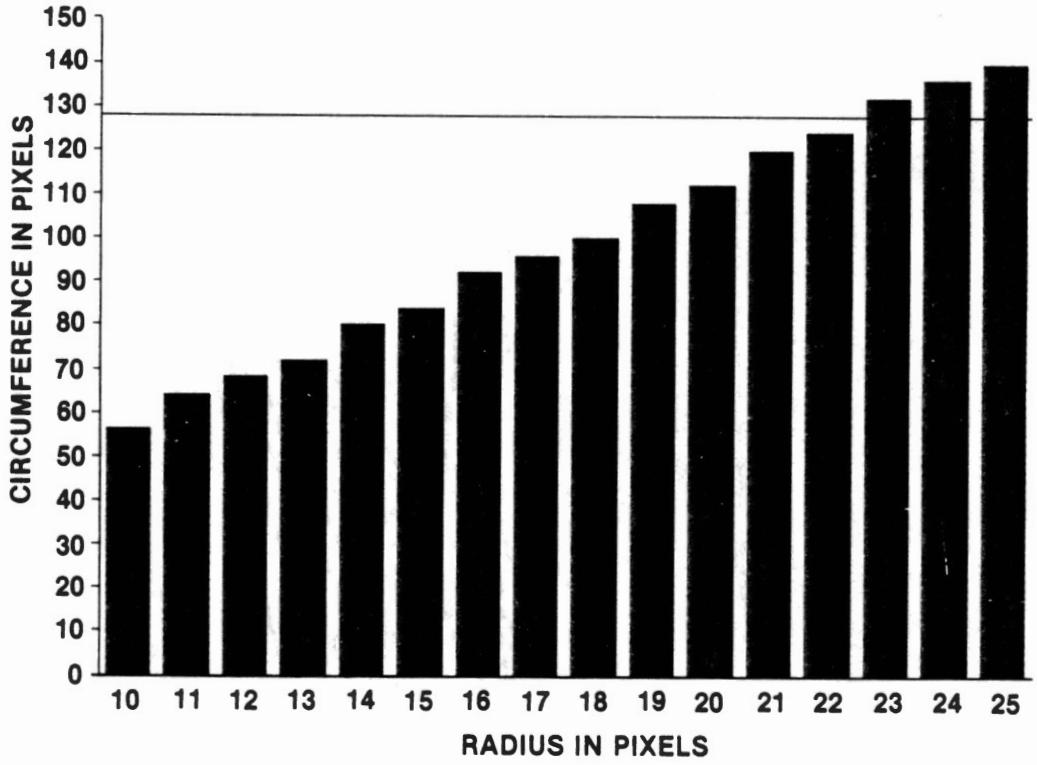

Figure 23. Polar Coordinate Resolution

required resolution. Pixels along the circumference of a diameter of 11 will appear, on the average, twice in the one-dimensional sequence.

Implementation of equation 3-36 is accomplished by using the Fast Fourier transform (FFT) algorithm. The FFT achieves a significant reduction in the number of computational steps over a direct implementation by exploiting the periodicity of the complex exponential. A listing and derivation of the FFT can be found in the textbook by Gonzales and Wintz (1977). An additional reduction by a factor of Q is possible since only the frequency components corresponding to an even multiple of 2π need be calculated. Moreover, a typical seedling usually has 15-20 needles, which suggests the use of a high-pass value. Implementing equation 3-36 used an initial value for u of 128.

The influence of foreign objects can be significantly reduced by initially high-pass filtering the image. Pine needles generally approximate bright lines of unit width. Convolving the image with the matrix,

$$\begin{bmatrix} -1 & -1 & -1 \\ -1 & 8 & -1 \\ -1 & -1 & -1 \end{bmatrix}$$

emphasizes the needles while simultaneously attenuating the influence of foreign objects. An example image corrupted by foreign objects and the corresponding transform are shown in Figures 24 and 25, respectively.

Figure 24. A Seedling Image Corrupted by Foreign Objects

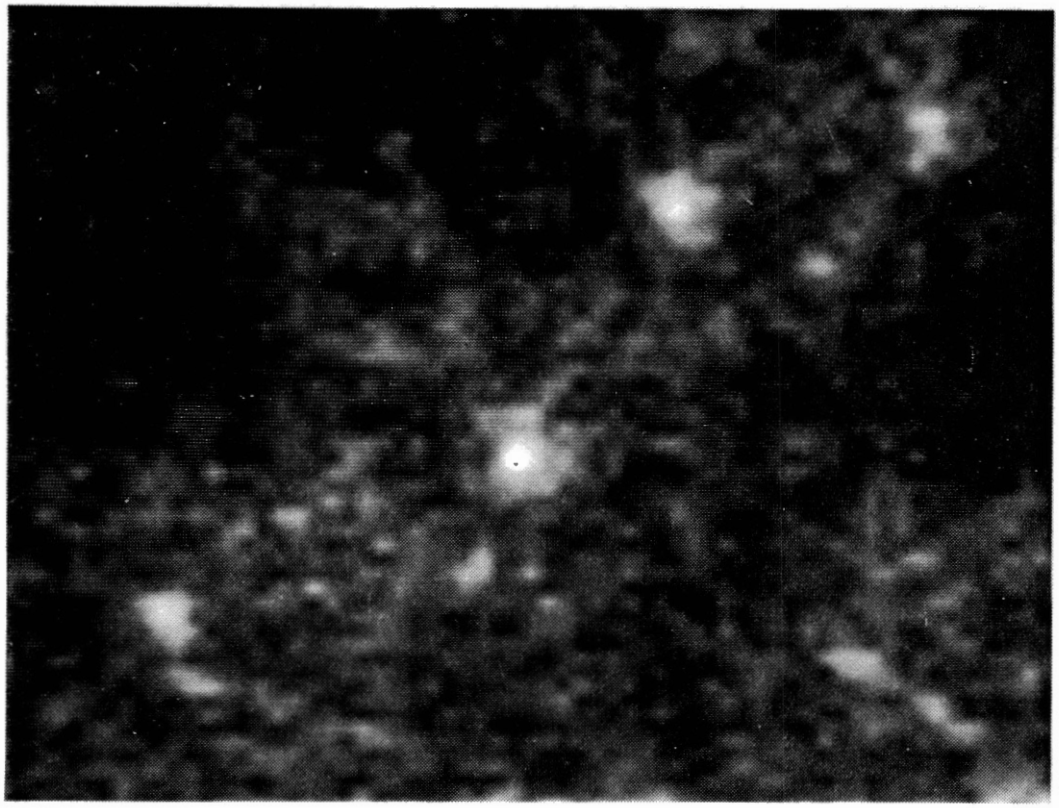

Figure 25. Transform of a Seedling Image Corrupted by Foreign Objects.

CHAPTER IV

ANALYSIS OF THE DATA

Twenty images were analyzed in an attempt to count pine seedlings. The camera was positioned approximately one meter above the seedlings, and an image was obtained by aiming the lens directly downward. Some images were purposely corrupted by introducing foreign objects such as grass and stones. A total of 121 trees were imaged, ranging from 2 to 11 trees per scene.

Individual seedlings are identified by locating bright spots in a transformed image defined by equation 3-36. The transformed image is converted into a binary image by global thresholding at a level calculated from the mode of a gray level histogram. The connect algorithm (chapter III) is used to identify separate connected regions of non-zero pixels in the binary image. Each region corresponds to a bright spot in the transformed image and is recognized as a seedling.

Results of the tests are summarized in Table I. Overall, about 93 percent of the seedlings were correctly identified. Errors occurred when a seedling was overlooked, or when a foreign object was identified as a seedling.

TABLE I

TEST RESULTS

Image	Seedlings	Extra	Missed	Error
1	3	1	0	1
2	5	0	0	0
3	8	0	0	0
4	9	0	1	1
5	8	0	0	0
6	3	0	0	0
7	8	0	0	0
8	9	0	1	1
9	3	0	0	0
10	7	0	0	0
11	11	0	1	1
12	5	0	0	0
13	9	1	1	2
14	3	0	0	0
15	2	0	0	0
16	5	0	1	1
17	4	0	0	0
18	6	0	0	0
18	9	0	0	0
20	4	0	1	1
TOTAL	121	2	6	8

Failure to detect a seedling was caused by obscured needles. In some images, seedlings were covered by larger adjacent seedlings. In other cases, needles were not straight, or they clumped together. Consequently, the surrounding region deviated from a radially symmetric function. An example of a seedling obscured by a larger seedling is shown in Figure 26.

False detection was caused by foreign objects such as thin blades of grass. When two or more blades of grass crossed, they formed a radially symmetric function. These types of objects hopelessly confound the data since they have features similar to pine needles. An example of false detection is shown Figure 27.

Failing to detect a seedling occurred more frequently than false detection. Foreign objects were positioned among different seedlings at random. As a result, the particular combination which resulted in a radially symmetric function occurred infrequently. A seedling partially occluded by either by a foreign object or another seedling was more likely to occur.

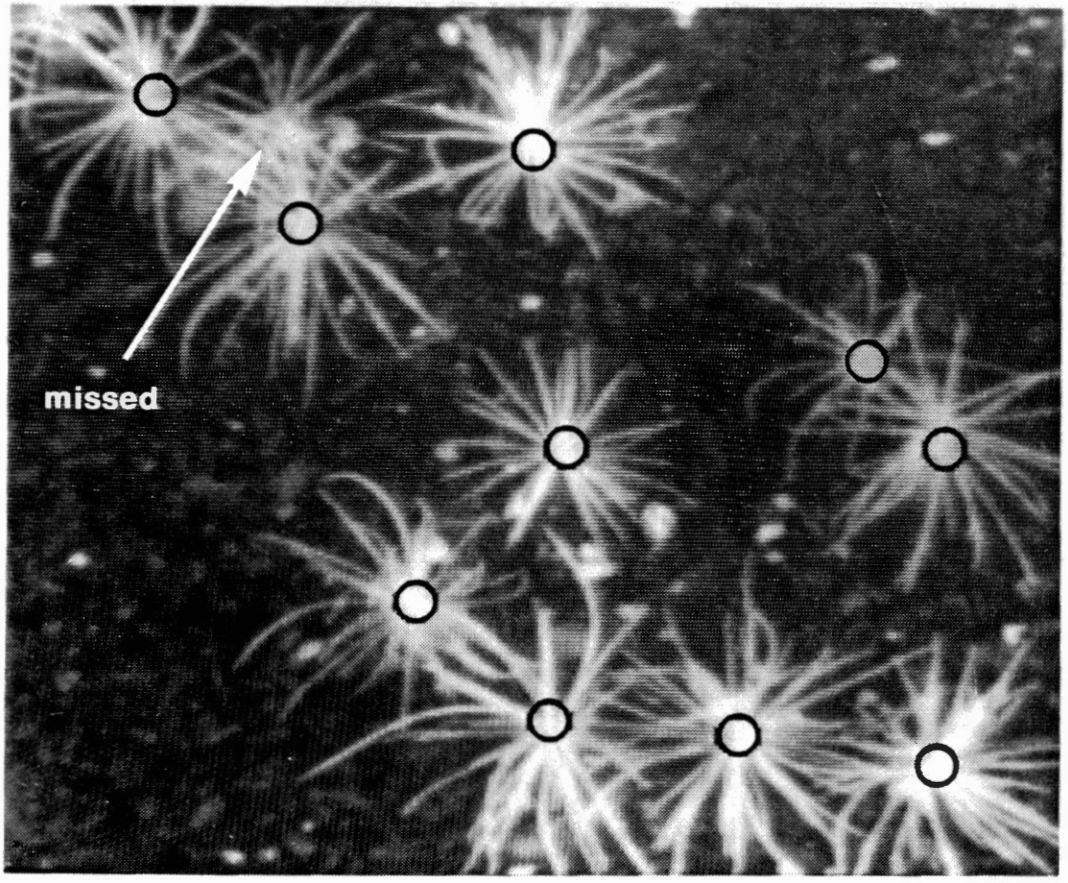

Figure 26. A Missed Seedling. The black circles identify detected seedlings.

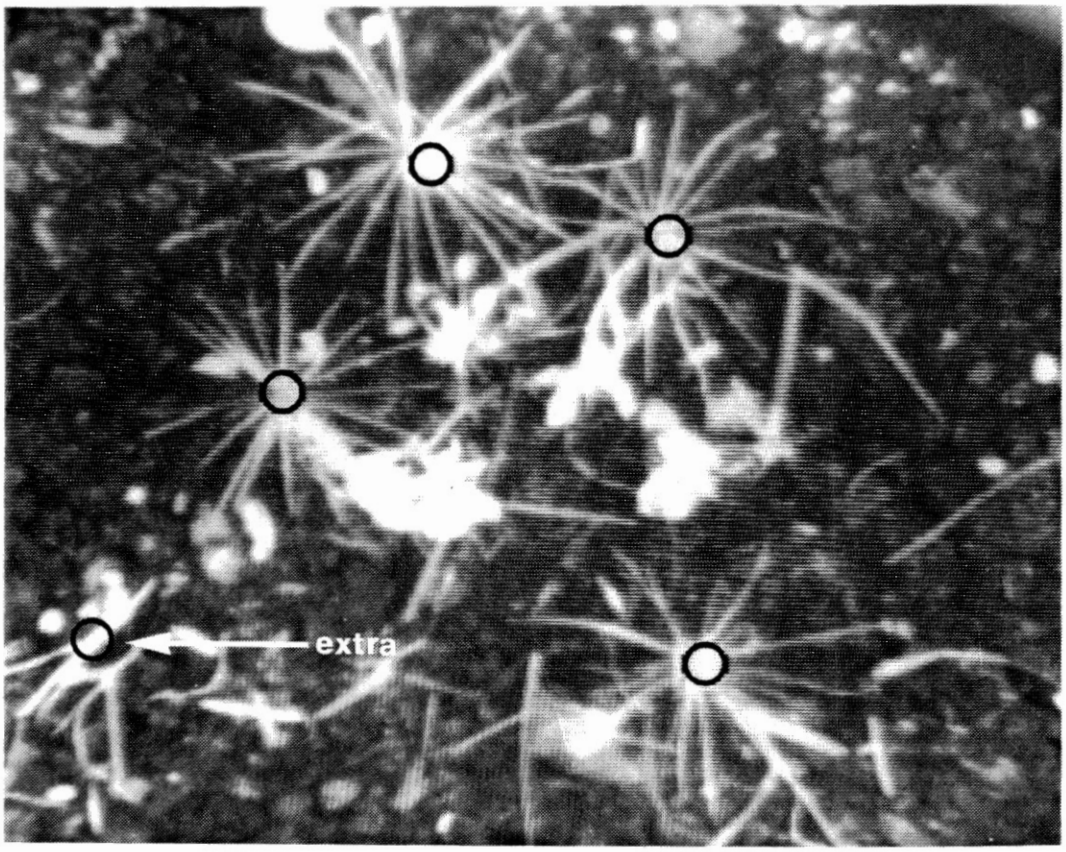

Figure 27. Detection Error. The black circles identify detected seedlings.

CHAPTER V

SUMMARY AND CONCLUSIONS

Summary

This dissertation is concerned with the development of an algorithm to detect pine seedlings in a digital image. The images are formed by a sensor which is positioned about one meter overhead the seedling bed. With this configuration, the seedlings appear as radially symmetric regions, characterized by pine needles which form radial lines.

Pine seedlings have three predominant features. The features are gray level contrast between seedling and background, lines formed by seedling needles, and the circular distribution of the needles. Four different algorithms are investigated.

To exploit the contrast between seedling and background, an algorithm to detect gray level peaks was developed. By increasing the camera's field-of-view, individual seedlings approximate circular bright spots. Low-pass filtering the image also helps to enhance the correlation between seedlings and gray level peaks. The number of gray level peaks indicates the number of seedlings.

Lines are detected by examining the spatial distribution of pixels which exhibit a low-high-low gray level transition. A line is defined to be a sequence of pixels whose locations obey the rules of a straight line beyond a minimum length. The geometric intersection of the lines identifies the location of a seedling center and thus provides a method to detect individual seedlings.

Gray level contour encoding makes use of contrast and lines. Contour encoding determines a sequence of pixel locations which enclose a region so that any pixel external to the region and adjacent to it will have a lower value than the boundary pixel. By selecting an appropriate gray level, pine needles will create a unique contour. Each needle will have a portion of the contour where the difference between locations on either side of the needle remains relatively constant over the length of the needle. Seedlings are identified as objects whose contours possess this trait.

An approach based on the Fourier transform exploits contrast, lines, and circular distribution. An annular region around a pixel is sampled according to a polar coordinate system. A one-dimensional sequence is formed by sampling pixels at a constant angular increment, from a minimum to maximum diameter. Pixels along a constant diameter are sampled, and the sequence is continued by sampling at the next larger diameter.

When the origin of the coordinate system coincides with the center of a seedling, the resulting sequence will be highly periodic. Moreover, since the sequence is radially symmetric, it will be completely described by frequencies which correspond to an even multiple of 2π. The discrete Fourier transform is calculated using only frequencies which are an even multiple of 2π.

The pixel at the centroid of the coordinate system is replaced by the maximum value of the energy spectrum. Repeating this procedure for each pixel in the image results in a transformed image which has large values near the center of a seedling. Isolating local maxima in the transformed image, either by gray level peaks, or simple global thresholding, enables individual seedlings to be detected.

Conclusions

The process of developing an algorithm investigates several different approaches. Some useful conclusions can be drawn from the investigation of each of these approaches.

The advantage of gray level peaks is speed and simplicity. Real-time implementation of this algorithm can be easily accomplished. With the exception of the connect() algorithm, the entire process can be implemented with a few parallel operations. Gray level peaks are also insensitive to global changes in gray level, since adding a constant value to F in equation 3-1 does not effect the result.

The disadvantage of using gray level peaks is susceptibility to foreign objects. Bright foreign objects could be incorrectly identified as seedlings. For controlled environments, gray level peaks may be useful, but on a broader scale the use of gray level peaks has limited application.

The use of lines to detect seedlings is predicated on the assumption that needles can be approximated by straight lines. In some cases, the needles curve, or a portion of the needle may be obscured. The chain-code is a liability for these cases because only a few missing pixels can completely disrupt a sequence.

Calculating geometric intersections with a digital computer is very tedious. Restricting the algorithm to line segments within a certain distance makes the the process excessively tedious, since the line data must be sorted for each coordinate. If the straight-line assumption is valid, a more feasible approach would be to use an optical technique.

An advantage of contour encoding is independence of specific image characteristics. As a result, the contour encoding approach should be useful over a variety of seedling images.

The limitation of gray level contour encoding is the inability to distinguish between closely spaced seedlings. Overlapping needles might cause the LML algorithm to "jump" over to the contour of an adjacent seedling.

The algorithm which uses the Fourier transform is the most complex technique. As a consequence, this algorithm is emphasized more than the previous techniques.

The process of approximating a sequence with a radially symmetric sequence can be accomplished in the frequency domain. In the spatial domain, the procedure amounts to calculating a mean value of the pixels at a specific angle. In the frequency domain, a radially symmetric approximation can be obtained by calculating the DFT of the one-dimensional sequence, and then zeroing all frequency coefficients which are not an even multiple of 2π.

The maximum energy value from the spectrum of a radial symmetric approximation is capable of distinguishing seedlings in noisy images. The energy value demonstrated successful detection with about 10 percent artificially added random noise. Noise tolerance is due, in part, to the independence of the maximum spectral value on the mean of the sequence.

The algorithm was implemented on an image processing system. The resolution of the system is inadequate for the size of a typical seedling. Increased spatial resolution should improve the performance of the algorithm, but the degree of improvement is unknown. Poor resolution did not inhibit the ability to detect pine seedlings.

Twenty sample images were analyzed. Results indicate that about 93 percent of the seedlings were correctly identified. The algorithm is particularly successful at detecting seedlings

within scenes containing a wide variety of foreign objects.

Problems occur when the needles are not distinct, or when foreign objects are radially symmetric. When needles are occluded or clumped together, the algorithm will fail to detect a seedling. When foreign objects are radially symmetric, such as overlapping blades of grass, the algorithm incorrectly identifies the foreign object as a seedling.

Recommendations for Further Research

A technique which employs more than one frequency coefficient may provide useful information. The number of needles per seedling is likely to be normally distributed. Statistics about several seedlings may provide a basis for a more selective frequency analysis.

The relationship between the spectra of adjacent pixels may help to detect seedlings. For a regular needle pattern, the spectrum of a sequence obtained slightly off-center will be a sinusoidal modulation of the spectrum obtained from an on-center sequence. The specific modulation should be similar regardless of the relative direction of the point off center. This approach becomes excessively complex when dealing with radial patterns which are not regular.

A system which implements the Fourier-based algorithm should make use of parallelism, yet minimize hardware costs. It is possible to design a system which would consist of a row of matrix sensors. Each sensor would have its own CPU and FFT

hardware. As the system is passed over the seedling bed, each sensor/CPU element simultaneously produces a maximum spectral value. Peak values indicate the sensor is directly over a seedling. While the concepts of such a system are valid, the cost would be prohibitive.

A more economical approach might use line scan sensors. Each line scan element could be mounted on a mechanically rotating base. If the rotational speed is much faster than the translational velocity, each discrete element would sweep out an approximate circle. Shifting out values from the line scan element at the appropriate time, would enable the calculation of the maximum spectral value.

A system based on gray level peaks would be the simplest and least expensive to implement. Assuming relative motion between the system and ground, continually shifting out values from a line scan sensor would provide an image matrix. An algorithm to locate gray level peaks would identify individual seedlings. The susceptibilty to foreign objects may not be a problem because the seedling beds are usually very clean. Hardware costs for such a system should be under $ 5000.

BIBLIOGRAPHY

Algar, V. S., H. Thiel. "Algorithm's for detecting M-dimensional objects in N-dimensional spaces." IEEE Trans. Pat. Anal. Mach. Intell., Vol. PAMI-3 (May, 1981), pp. 245-256.

Arakawa, K., K. Odata, T. Masuada. "On-line recognition of hand-written characters -- alphanumerics, hiranga, katakana, kanji." Proc. 4th Intl. Conf. Pattern Recognition. Kyoto, Japan: IAPR, Nov. 7-10, 1978, pp. 810-812.

Arcelli, C., A. Massarotti. "Regular arcs in digital contours." Comput. Graphics, Image Processing, Vol. 4 (1975), pp. 339-360.

Asada, H., M. Brady. "The curvature primal sketch." IEEE Trans. Pat. Anal. Mach. Intell., Vol. PAMI-8, No. 1 (Jan., 1986). pp. 2-14.

Attneave, F. "Some informational aspects of visual perception." Psychol. Rev., Vol. 61 (1954), pp. 183-193.

Babuad, J., A. P. Witkin, M. Baudin, R. O. Duda. "Uniqueness of the guassian kernal for scale space filtering." IEEE Trans. Pat. Anal. Mach. Intell., Vol. PAMI-8, No. 1 (Jan., 1986). pp. 26-33.

Bacus, J. W., E. E. Gose. "Leucocyte pattern recognition.", IEEE Trans. Syst., Man, Cybern., Vol. SMC-2 (1974), pp. 513-526.

Ballard, D. H. "Generalizing the Hough transform to detect arbitrary shapes." Pat. Recognition, Vol. 13 (1981), pp. 111-112.

Bartz, M. R. "Optimizing a video processor for OCR." Artificial Intelligence Int'l. Joint Conf. Proc.. Bedford: Mitre Corp., 1969, pp. 79-90.

Baylou, P., B. El Hadj Amor, G. Bousseau, "Automatic recognition of moving objects and its application to a robot for picking asparagus." Proc. SPIE, Vol. 397 (1983), pp. 234-239.

Bennet, J. R., J. S. McDonald. "On the measurements of curvature in a quantized environment." IEEE Trans. Comput., Vol. C-24 (1975), pp. 803-820.

Berlage, A. G., T. M. Cooper, R. A. Carone. "Seed recognition potential of machine vision." (Unpublished paper No. 84-3059 presented at Am. Soc. Agr. Engr. meeting, Knoxville, Tenn., June 24-27, 1984.)

Bhanu, B., O. D. Fuageras. "Shape matching of two-dimensional objects." IEEE Trans. Pat. Anal. Mach. Intell., Vol. PAMI-6, No. 2 (Mar. 1984), pp. 137-144.

Bjorklund, C. M., T. Pavlidis. "Global shape analysis by K-syntatic similarity." IEEE Trans. Pat. Anal. Mach. Intell., Vol. PAMI-3 (Mar. 1981), pp. 144-155.

Blum, H. "A transformation for extracting new descriptors "of shape." Symposium on Models for the Perception of Speech and Visual Form, Boston: M.I.T. Press, 1964.

Blum, H., R. Nagel. "Shape description using weighted symmetric axis features." Proc. IEEE Pattern Recognition and Image Processing Conf. Troy, N.Y.: June 6-8, 1977, pp. 203-215.

Boeckman, B. Personal Interview. Fort Towson, Oklahoma, May, 1984.

Brons, R. "Linguistic methods for the description of a straight line on a grid." Comput. Graphics, Image Processing, Vol. 3 (1974), pp. 48-62.

Brown, C. M., "Inherent bias and noise in the Hough transform." IEEE Trans. Pat. Anal. Mach. Intell., Vol. PAMI-5, No. 5 (Sep., 1983).

Calabi, L., W. E. Hartnett. "Shape recognition, prairie fires, convex deficiencies and skeletons." Am. Math Monthly, Vol. 75, No. 4 (Apr., 1968), pp. 335-342.

Chaudhuri, B. B. "Applications of quadtree, octree, and binary tree decomposition techniques to shape analysis and pattern recognition." IEEE Trans. Pat. Anal. Mach. Intell., Vol. PAMI-7, No. 6 (Nov. 1985), pp. 652-661.

Chellappa, R., R. Bagdazain. "Fourier coding of image boundaries." IEEE Trans. Pat. Anal. Mach. Intell., Vol. PAMI-6, No. 1 (Jan., 1984), pp. 102-105

Chomsky, N. Syntactic Structures. 4th Ed. Hague: Mouton Pub. Co., 1964.

Chow, C. K., T. Kaneko. "Boundary detection of radiographic images by a threshold method." Proc. IFIP Congress 71 Booklet TA-7: Amsterdam, 1972, pp. 130-134.

Cooley, J. W., J. W. Tukey. "An algorithm for machine calculation of complex Fourier series." Math. of Comput., Vol. 19 (1965), pp. 297-301.

DaSilva, F., D. L. Thomas, A. Shimohammadi, W. A. Cromer. "Development of a plant growth evaluation technique through computer based image processing." (Unpublished paper No. 85-3547 presented at Am. Soc. Agr. Engr. meeting, Chicago, Il., Dec. 17-20, 1985.)

Danker, A. J., A. Rosenfeld. "Blob detection by relaxation." IEEE Trans. Pat. Anal. Mach. Intell., Vol. PAMI-3, No. 1 (Jan., 1981).

Davis, L. S. "A survey of edge detection techniques." Computer Graphics and Image Processing, Vol. 4 (1974), pp. 248-270.

Davis, L. S., "Understanding shape: angles and sides." IEEE Trans. Comput., Vol. C-26 (1977), pp. 236-242.

Deans, S. "Randon transform related to Hough transform; application to line and curve detection in digital images." IEEE Trans. Pat. Anal. Mach. Intell., Vol. PAMI-3 (Mar., 1981), pp. 185-188.

Deutsch, S. "Conjectures on mammalian neuron networks for visual pattern recognition." IEEE Trans. Syst., Sci., Cybern., Vol. SSC-2 (Dec., 1966), pp. 81-85.

Dodd, G. G., W. A. Perkins. "Computer vision proves viable for inspecting assembly-line parts." Computer Technology Review, Vol. 3, No. 1 (Jan., 1983), pp. 363-366.

Dondes, P. A., A. Rosenfeld. "Pixel classification based on gray level and local busyness." IEEE Trans. Pat. Anal. Mach. Intell., Vol. PAMI-4, No. 1 (Jan., 1982).

Dorst, L., R. P. W. Duin. "Spirograph theory: a framework for calculations on digitized straight lines." IEEE Trans. Pat. Anal. Mach. Intell., Vol. PAMI-6, No. 5 (Sep., 1984), pp. 632-639.

Dorst, L., A. W. M. Smeulders. "Discrete representation of straight lines." IEEE Trans. Pat. Anal. Mach. Intell., Vol. PAMI-6, No. 4 (Jul., 1984), pp. 450-463.

Doyle, W. "Operations useful for similarity invariant pattern recognition." J. Assoc. Computing Mach., Vol. 9 (1962), pp. 259-257.

Dubois, S. R., F. H. Glanz. "An autoregresion model approach to two-dimensional shape classification." IEEE Trans. Pat. Anal. Mach. Intell., Vol. PAMI-8, No. 1 (Jan., 1986). pp. 55-66.

Duda, R. O., P. E. Hart. Pattern Classification and Scene Analysis. New York: Wiley Pub. Co., 1971.

Duda, R. O., P. E. Hart. "Use of Hough transform to detect lines and curves in pictures." Commun. Ass. Comput. Mach., Vol. 15 (Jan. 1972), pp. 11-15.

Dudani, S. A., K. J. Breedy, R. B. McGhee. "Aircraft classification by the moment invariants." IEEE Trans. Comput., Vol. C-26 (1977), pp. 39-46.

Eccles, M. J., P. C. McQeens, D. Rosen. "Analysis of the digitized boundaries of planar objects." Pattern Recognition, Vol. 9 (1977), pp. 31-41.

Eguchi, H., M. Hanakoga, T. Matsui. "Computer control of plant growth by image processing. IV. Digital image processing of reflectance in different wave length regions of light for evaluating vigor of plants." Environ Control in Biol., Vol. 17, No. 2 (1979), pp. 67-77.

Eguchi, H., T. Matsui. "Computer control of plant growth by image processing. II. Pattern recognition of growth in on-line system. Environ Control in Biol., Vol. 15, No. 2 (1977), pp. 37-45.

Eguchi, H., T. Matsui. "Computer control of plant growth by image processing. III. Image processing for evaluation of plant growth in practical cultivation." Environ Control in Biol., Vol. 16, No. 2 (1978), pp. 47-55.

Feder, J. "Languages of encoded line patterns." Inf. Control, Vol. 13 (1968), pp. 230-244.

Feivson, A. "Classification by thresholding." IEEE Trans. Pat. Anal. Mach. Intell., Vol. PAMI-5, No. 1 (Jan., 1983).

Fischler, M. A., R. C. Bolles. "Perceptual organization and curve partitioning." IEEE Trans. Pat. Anal. Mach. Intell., Vol. PAMI-8, No. 1 (Jan., 1986). pp. 100-105.

Freeman, H. "On the encoding of arbitrary geometric configurations." IRE Trans. Electron. Comput., Vol. EC-10 (June, 1961), pp. 260-268.

Freeman, H. "Boundary encoding and processing." Picture Processing and Psychopictorics. Eds. B. S. Lipkin and A. Rosenfeld. New York: Academic Press, 1970, pp. 241-266.

Freeman, H. "Application of the generalized coding scheme to map data processing." Proc. IEEE Pattern Recognition and Image Processing Conf. Chicago: May 31-June 2, 1978, pp. 220-226.

Freeman, H. "Shape discrimination via the use of critical points." Pattern Recognition, Vol. 10 (1978), pp. 159-166.

Freeman, H., A. Saghri. "Generalized chain codes for planar curves." Proc. 4th Intl. Joint Conf. Pattern Recognition. Kyoto, Japan: IAPR, Nov. 7-10, 1978, pp. 701-703.

Frischkopf, L. S., L. D. Harmon. "Machine reading of cursive script." Proc. Symposium on Information Theory. London: Butterworth, Ed. C. Cherry, 1961, pp. 300-316.

Frost and Sullivan, Inc. U.S. Commercial Market for Image Processing Systems. New York: N.Y., Technical report No. A1499, 1986.

Fu, K. S. Syntactic Pattern Recognition and Applications. Eds. Aliza Greenblett. Englewood Cliffs, N. J. : Prentice-Hall, Inc., 1982.

Fu, K. S. "Pattern recognition for automatic visual inspection." Computer, Vol. 15, No. 12 (1982), pp. 34-40.

Fu, K. S., J. K. Mui. "A Survey on image segmentation." Pattern Recognition, Vol. 13 (1981), pp. 3-16.

Gaafar, M. "Convexity verification, block chords, and digital straight lines." Comput. Graphics, Image Processing, Vol. 6 (1977), pp. 361-370.

Gerrish, J. B., T. C. Surbrook. "Mobile robots in agriculture." Robotics and Intelligent Machines in Agriculture, St. Joseph, MI., ASAE Pub. 4-84 (1984), pp.30-41.

Gold, M. "Voyager to the seventh planet." Science 86, Vol. 7, No. 4 (May, 1986). pp. 32-39.

Gonzales, R. and P. Wintz. Digital Image Processing. 6th Ed. Reading, Massachusetts: Addison-Wesley Publishing Co., Inc., 1977.

Goodman, J. W. Introduction To Fourier Optics. 1st Ed. San Franciso, CA: Mcgraw-Hill Book Co., Inc., 1968, p. 27

Goshtasby, A. "Description and discrimination of planar shapes using shape matrices." IEEE Trans. Pat. Anal. Mach. Intell, Vol. PAMI-7, No. 6 (Dec. 1985), pp. 738-743.

Grand d'Esnon, A. "Robotic harvesting of apples." Robotics and Intelligent Machines in Agriculture, St. Joseph, MI., ASAE Pub. 4-84 (1984). pp. 112-113.

Granlund, G. H. "Fourier preprocessing for hand print character recognition." IEEE Trans Comput., Vol. C-21 (1972), pp. 195-201.

Griffith, A. K. "Edge detection in simple scenes using a priori information." IEEE Trans. Comput., Vol. C-22, No. 4 (April, 1973), pp. 371-381.

Griffith, A. K. "Mathematical models for automatic line detection." J. Ass. Comput. Mach., Vol. 20, No. 1 (Jan., 1973), pp. 62-80.

Gritton, C. W. K., E. A. Parrish, Jr. "Boundary location from an initial plan: The bead chain algorithm." IEEE Trans. Pat. Anal. Mach. Intell., Vol. PAMI-5, No. 1 (Jan., 1983).

Groen, F. C. A., P. W. Verbeek. "Freeman-code probabilities of object boundary quantized contours." Comput. Graphics, Image Processing, Vol. 7 (1977), pp. 391-402.

Guyer, D. E., G. E. Miles, M. M. Schreiber. "Computer vision and image processing for plant identification." (Unpublished paper No. 84-1632 presented at Am. Soc. Agr. Engr. meeting, New Orleans, Lo., Dec., 1984.)

Hall, R. C. Lunar Impact - A history of project ranger. Washington: U. S. Government Printing Office, 1977.

Harrel, R. C., P. D. Adsit, D. C. Slaughter. "Real-time vision servoing of a robotic tree fruit harvester." (Unpublished paper No. 85-3550 presented at Am. Soc. Agr. Engr. meeting, Chicago, Il., Dec. 17-20, 1985)

Hildreth, E. Edge Detection. Artifical Intell. Lab Memo No. 858. Boston: Mass. Inst. Tech., Sep., 1985.

Hong, T. H., A. Rosenfeld. "Compact region extraction using weighted pixel linking in a pyramid." IEEE Trans. Pat. Anal. Mach. Intell., Vol. PAMI-6, No. 2 (Mar. 1984), pp. 222-229.

Hong, T. H., M. Shneier. "Extracting compact objects using linked pyramids." IEEE Trans. Pat. Anal. Mach. Intell., Vol. PAMI-6, No. 2 (Mar. 1984), pp. 229-237.

Hough, P. V. C. " Method and means for recognizing complex patterns." U. S. Patent 3,069,654, 1962.

Hu, M. "Visual pattern recognition by moment invariants." IRE Trans. Inform. Theory, Vol. IT-8 (Feb., 1962), pp. 179-187.

Hubel, D. H., T. N. Wiesel. "Receptive fields, binocular interaction and functional architecture in the cat's visual cortex." J. Physiol., Vol. 160 (1962), pp. 106-154.

Hudson, D. L. " Food for thought and appearance." Proc. of the Third Annual Applied Machine Vision Conference. Chicago: Octeck, Inc., Feb 27 - Mar 1, 1984.

Hueckel, M. F. "An operator which locates edges in digitized pictures." J. Assoc. Comput. Mach., Vol. 18 (Jan. 1971), p 113-125.

Hueckel, M. F. "A local operator which recognizes edges and lines." J. Assoc. Comput. Mach., Vol. 20 (1973), pp. 634-647.

Huffman, D. A. "A method for the construction of minimum redundancy codes." Proc. IRE, Vol. 40, No. 10 (1952), pp. 1098-1101.

Hung, S. H. Y. "On the straightness of digital arcs." IEEE Trans. Pat. Anal. Mach. Intell., Vol. PAMI-7, No. 2 (Mar. 1985), pp. 203-215.

Ito, T. "Pattern classification by color effect method." Proc. Second Int'l. Joint Conf. Pattern Recognition. Aug., 1974, pp. 76-77.

IRI. IKS Manual. International Robomation/Intelligence, 2281 Las Palmas Drive, Carlsbad, CA., 92008. 1985.

Jacobs, C. J., R. T. Chein. "Two new edge detectors." IEEE Trans. Pat. Anal. Mach. Intell., Vol. PAMI-3, No. 5 (Sep., 1981), pp. 581-592.

Jarvis, J. F. "Regular expression as a feature selection language for pattern recognition." Proc. 3rd Intl. Joint Conf. Pattern Recognition. Coronado, CA.: Nov., 1976, pp. 189-192.

Jepsen, P. L., J. A. Mosher, G. M. Yagi, C. C. Avis, G. W. Garneau, J. J. Lorre, E. P. Korsmo, and L. R. Doyle. "Application of image processing to voyager imagery." Proc. SPIE, Vol. 292 (1981).

Kim, C. E. "On cellular straight line segments." Comput. Graphics Image Process., Vol. 18 (1982), pp. 369-381.

Kim, C. E., A. Rosenfeld. "Digital straight lines and convexity of digital regions." IEEE Trans. Pat. Anal. Mach. Intell, Vol. PAMI-4 (1982), pp. 149-153.

Kimme, C., D. Ballard, J. Sklansky. "Finding circles by an array of accumulators." Commun. Ass. Comput. Mach., Vol. 18, No. 2 (1975), pp. 120-122.

Kinnucan, P. "Machines that see." High Technology, Vol. 3, No. 4 (April, 1983), pp. 30-36.

Kirsh, R. "Computer determination of the constituent structure of biological images." Computer and Biomedical Research, Vol. 4, No. 3 (1971), pp. 315-328.

Klinger, A. "Minimal quadtrees." Proc. 7th Intl. Conf. Pattern Recognition. Montreal: CIPPR Soc., Jul. 30 - Aug. 2, 1984, pp. 814-816.

Knoke, P. J., R. G. Wiley. "A linguistic approcah to mechanical pattern recognition." Proc. IEEE Comput. Conf. Sep., 1967, pp. 142-144.

Koplowitz, J. "On the performance of chain codes for quantization of line drawings." IEEE Trans. Pat. Anal. Mach. Intell., Vol. PAMI-3 (Mar., 1981), pp. 180-185.

Kranzler, G. A. "Applying digital image processing in agriculture." Agricultural Engineering, Vol. 66, No. 3 (1985), pp. 11-13

Ledley, R. S. "High-speed automatic analysis of biomedical pictures." Science, Vol. 146, No. 3461 (1964), pp. 216-213.

Lee, H. C., K. S. Fu. "Using the FFT to determine digital straight line chain codes." Comput. Graphics Image Processing, Vol. 18 (1982), pp. 359-368.

Leroi, M., M. Burton. "Structural encoding of linear outlines in scene analysis." Proc. 5th Int. Conf. Pattern Recognition. Dec., 1980, pp. 358-360.

Marr, D. Analyzing natural images; a computation theory of texture vision. Boston: Mass. Inst. Tech. AI Lab, Tech. report 334, June, 1975.

Mayo, W. T., Jr. "On-line analyzers help machines see." Instruments and Control Systems, Vol. 55, No. 8 (1982).

McClure, D. E. "Nonlinear segmented function approximation and analysis of line patterns." Quant. Appl., Vol. 33 (1975), pp. 1-37.

McFarlane, M. D. "Digital pictures fifty years ago." Proc. of IEEE, Vol. 60, No. 7 (1972).

Mckee, J. W., J. K. Aggarwl. "Computer recognition of partial views of curved objects." IEEE Trans. Comput., Vol. C-26 (1977), pp. 790-800.

Mero, L. "Line-following algorithm for digitized T.V. pictures." IEEE Trans. Pat. Anal. Mach. Intell., Vol. PAMI-3 (Sep., 1981). pp. 593-598.

Meyer, G., D. A. Davison. "An electronic image plant growth measurement system." (Unpublished paper No. 85-3548 presented at Am. Soc. Agr. Engr. meeting, Chicago, Il., Dec. 17-20, 1985)

Minami, T., K. Shinohara. "Encoding of line drawings with a multiple grid chain code." IEEE Trans. Pat. Anal. Mach. Intell., Vol. PAMI-8, No. 2 (Mar., 1986), pp. 269-276.

Minor, L. G., J. Sklansky. "The detection and segmentation of blobs in infrared images." IEEE Trans. Syst., Man, Cybern., Vol. SMC-11 (Mar., 1981), pp. 194-201.

Mokhtarian, F. A. Mackworth. "Scale-based description and recognition of planar curves and two-dimensional shapes." IEEE Trans. Pat. Anal. Mach. Intell., Vol. PAMI-8, No. 1 (Jan., 1986). pp. 34-43.

Montanari, V. "Continuous skeletons from digital images." J. Assoc. Comput. Mach., Vol. 16 (1969), pp. 534-549.

Nagy, G. "Feature extraction on binary patterns." IEEE Trans. Syst., Sci., Cybern., Vol. SSC-5 (1969), pp. 273-278.

Nevatia, R. "Locating object boundaries in textured environments." IEEE Trans. Comput., Vol. C-25, No. 11 (Nov., 1976), pp. 1170-1175.

O'Gorman, L., A. C. Sanderson. "The converging squares algorithm : An efficient method for locating peaks in multi-dimensions." IEEE transactions Pat. Anal. Mach. Intell., Vol. PAMI-7 (May, 1984), pp. 280-288.

Ohlander, R., K. Price, R. Reddy. "Picture segmentation using a recursive region splitting method." Comput. Graphic., Image Processing, Vol. 8 (1978), pp. 313-333.

Pavlidis, T. "Analysis of set patterns." Pattern Recognition, Vol. 1 (1968), pp. 165-178.

Pavlidis, T. "Computer recognition of figures through decomposition." Inform. Control, Vol. 14 (1968), pp. 526-537.

Pavlidis, T. "Polygon approximations by Newton's method." IEEE Trans. Comput., Vol. C-26 (1977), pp. 800-807.

Pavlidis, T. "A review of algorithms for shape analysis." Comput. Graph. Image Processing, Vol. 7 (1978), pp. 243-256.

Pavlidis, T. "A thinning algorithm for discrete binary images." Comput. Vision, Graph., Image Processing, Vol. 13 (1980), pp. 142-157.

Pavlidis, T. "Algorithms for shape analysis of contours and waveforms." IEEE Trans. Pat. Anal. Mach. Intell., Vol. PAMI-2 (Jul., 1980), pp. 301-312.

Pavlidis, T., S. L. Horowitz. "Segmentation of plane curves." IEEE Trans. Comput., Vol. C-23 (1974), pp. 860-870.

Peli, T. "An algorithm for recognition and localization of rotated and scaled objects." Proc. IEEE, Vol. 69, No. 4 (1981), pp. 483-485.

Perkins, W. A. "A model-based vision system for industrial parts." IEEE Trans. Comput., Vol. C-27 (1978), pp. 126-143.

Perkins, W. A. "Area segmentation of images using edge points." IEEE Trans. Pat. Anal. Mach. Intell., Vol. PAMI-2 (Jan., 1980), pp. 8-15.

Persoon, E., K. S. Fu. "Shape discrimination using Fourier descriptors." Proc. 2nd Intl. Conf. Pattern Recognition. Copenhagen: 1974, pp. 126-130.

Persoon, E., K. S. Fu. "Shape discrimination using Fourier descriptors." IEEE Trans. Syst., Man, Cybern., Vol. SMC-7 (1977), pp. 170-179.

Pope, R. "Computer with eyes." Industrial Research and Development, (May, 1978), pp. 105-108.

Pratt, W. K. Digital Image Processing. 1st Ed. New York: John Wiley & Sons, Inc., 1978.

Prewitt, J. M. S., M. L. Mendelsohn. "The analysis of C images." Ann. N. Y., Aead. Sci., Vol. 128 (1966), pp. 1035-1053.

Radon, J. "Uber die bestimmung von funktionen durch ihre integralwerte langs gewiser mannigfaltigkeiten." Ber. Saechs. Akad. Wiss. Leipzig, Math-Phys. Kl., Vol. 69 (Apr., 1917), pp. 262-277.

Ranade, S., M. Shneier. "Using quadtrees to smooth images." Proc. 5th Intl. Conf. Pattern Recognition. Miami: IEEE Comput. Soc., Dec. 1-4, 1980, pp. 811-814.

Rice, J. R. The Approximation of Functions. Vol. 2, New York: Addison Wesly, 1969, Ch. 10.

Roberts, L. G. "Machine perception of three dimensional solids." Optical and Electro-Optical Information Processing. Eds. J. T. Tippet. Cambridge, Mass. : MIT Press, 1965.

Robinson, G. S. "Detection and coding of edges using directional masks." Proc. of SPIE Conf. on Advances in Image Transmission Techniques. San Diego: Aug., 1976.

Rosenfeld, A. "A nonlinear edge detection technique." Proc. IEEE Letters, Vol. 58, No. 5 (May, 1970), pp. 814-816.

Rosenfeld, A. "Compact figures in digital pictures." IEEE Trans. Syst., Man, Cybern., Vol. SMC-4 (1974), pp. 211-223.

Rosenfeld, A. "Digital straight line segments." IEEE Trans. Comput., Vol. C-23 (1974), pp. 1264-1269.

Rosenfeld, A. "Relaxation methods in image processing and analysis." Proc. 4th Intl. Conf. Pattern Recognition. Kyoto, Japan: IAPR, Nov. 7-10, 1978, pp. 181-185.

Rosenfeld, A. "Quadtree and pyramids for pattern recognition and image processing." Proc. 5th Intl. Conf. Pattern Recognition. Miami: IEEE Comput. Soc., Dec. 1-4, 1980, pp. 802-811.

Rosenfeld, A., A. Kak. Digital Picture Processing. 2nd Ed. Ed. Werner Rheinboldt. New York: Academic Press, 1976, pp. 211-219.

Rosenfeld, A., E. Johnston. "Angle detection on digital curves." IEEE Trans. Comput., Vol. C-22 (1973), pp. 874-878.

Rosenfeld, A., J. L. Pfaltz. "Sequential operations in digital picture processing." J. Assoc. Comput. Mach., Vol. 13 (1966), pp. 471-494.

Rosenfeld, A., M. Thurston. "Edge and curve detection for visual scene analysis." IEEE Trans. Comput., Vol. C-20 (May, 1971), pp. 562-569.

Rutkowski, W. S., S. Peleg, A. Rosenfeld. "Shape segmentation using relaxation." IEEE Trans. Pat. Anal. Mach. Intell., Vol. PAMI-3, (Jul., 1981), pp. 368-375.

Rutovitz, D. "Centromere finding: Some shape descriptors for small chromosome outlines." Machine Intell., Vol. 5 (1970), pp. 435-462.

Saghri, J. A., H. Freeman. "Planar curve representation using chain codes; quantization error." IEEE Trans. Pat. Anal. Mach. Intell., Vol. PAMI-3 (Sep., 1981), pp. 533-539.

Samet, H. "Approximation and compression of images using quadtrees." Proc. 7th Intl. Conf. Pattern Recognition. Montreal: CIPPR Soc., Jul. 30-Aug. 2, 1984, pp. 220-223.

Samet, H., R. E. Webber. "On encoding boundaries with quadtrees." IEEE Trans. Pat. Anal. Mach. Intell., Vol. PAMI-6, No. 3 (May, 1984).

Sarkar, N., R. R. Wolfe. "Feature extraction techniques for sorting tomatoes by computer vision." Trans. of ASAE, Vol. 28, No. 3. (1985), pp. 970-974.

Searcy, S. W., J. F. Reid. "Detecting Crop Rows Using the Hough Transform." (Unpublished paper No. 86-3042 presented at Am. Soc. Agr. Engr. meeting, San Luis Obispo, CA, June, 1986)

Shahraray, B., D. Anderson. "Uniform resampling of digitized contours." IEEE Trans. Pat. Anal. Mach. Intell., Vol. PAMI-7, No. 6 (1985), pp. 674-681

Shaw, A. C. "Parsing of graph-represented pictures." J. Assoc. Comput. Mach., Vol. 17, No. 3 (1970), pp. 453-481.

Shneier, M. "Using pyramids to define local thresholds for blob detection." IEEE Trans Pat. Anal. Mach. Intell., Vol. PAMI-5, No. 3 (May, 1983).

Sistler, F. E., P. A. Smith, D. C. Rester. "An image analyzer for aerial application patterns." Trans. ASAE, Vol. 25, No. 4 (1982), pp. 885-887.

Sloan, K. R. Jr., D. H. Ballard. "Experience with the generalized Hough transform." Proc. 5th Int. Conf. Pat. Recognition. Miami: IEEE Comput. Soc., Dec 1-4, 1980, pp. 174-179.

Sloan, K. R., Jr. "Analysis of dot product shape descriptions." IEEE Trans Pat. Anal. Mach. Intell., Vol. PAMI-4, No. 1 (Jan. 1982).

Stark, H. "Polar Sampling Theorems of use in Optics." Proc. SPIE on Application of Math. Mod. Optics, Vol. 358 (1982), pp. 24-30.

Strackee, J., N. J. D. Nagelkerke. "On closing the Fourier descriptor presentation." IEEE Trans. Pat. Anal. Mach. Intell., Vol. PAMI-5, No. 6 (Nov., 1983).

Tabatabai, A. J., O. R. Mitchell. "Edge location to subpixel vales in digital imagery." IEEE Trans. Pat. Anal. Mach. Intell., Vol. PAMI-6, No. 2 (Mar., 1984), pp. 188-201.

Titchmarsh, E. C. Introduction to Theory of Fourier Integrals. New York: Oxford Univ. Press., 1948.

Tsai, W., S. Yu. "Attributed string matching with merging for shape recognition." IEEE Trans. Pat. Anal. Mach. Intell, Vol. PAMI-7, No. 4 (Jul., 1985), pp. 453-462.

Turney, J. L., T. N. Mudge, R. A. Voltz. "Recognizing partially occluded parts." IEEE Trans. Pat. Anal. Mach. Intell., Vol. PAMI-7, No. 4 (July, 1985).

Wagner, J. N. "Inspecting the impossible." Food Engineering, Vol. 55, No. 6 (June, 1983), pp. 79-92.

Wahl, F. M. "A new distance mapping and its use for shape measurement on binary patterns." Comput. Vision, Graph., Image Processing, Vol. 23 (1983), pp. 218-226.

Weska, J. S. "A survey of threshold selection techniques." Computer Graphics and Image Processing, Vol. 7 (1978), pp. 259-265.

Weska, J. S., R. N. Nagel, A. Rosenfeld. "A threshold selection technique." IEEE Trans. Comput., Vol. 23 (1974), pp. 1322-1326.

Whittaker, A. D., G. E. Miles, O. R. Mitchell, L. D. Gaultney. "Fruit location in a partially occluded image." (Unpublished paper No. 84-5511 presented at Am. Soc. Agr. Engr. meeting, New Orl. LO., Dec., 1984.)

Wu, L. D. "On the Freeman's conjecture about the chain code of a line." Proc. 5th Int. Conf. Pattern Recognition. Miami: IEEE Comput. Soc., Dec. 1-4, 1980, pp. 32-34.

Wu, L. D. "On the chain code of a line." IEEE Trans. Pat. Anal. Mach. Intell., Vol. PAMI-4 (1982), pp. 347-353.

Yogendra, J. T., R. A. Jones. "Machine recognition of partial shapes using feature vectors." IEEE Trans. Syst., Man, Cybern., Vol. SMC-15, No. 4 (Jul./Aug., 1984).

Yoshio, I., R. Yamashita, Y. Matsuo. "On the system evaluating the shape of farm products via image processing technique (Part 1)." J. Society of Agr. Mach., No. 48, 49 (1980), pp. 76-77, 48-52.

Yuille, A. L., T. A. Poggio, "Scaling theorems for zero crossings." IEEE Trans. Pat. Anal. Mach. Intell., Vol. PAMI-8, No. 1 (Jan., 1986). pp. 15-25.

Zabelle, G. S., J. K. Koplowitz. "Fourier encoding of closed planar boundaries." IEEE Trans. Pat. Anal. Mach. Intell., Vol. PAMI-7 (Jan. 1985), pp. 98-102.

Zahn, C. T., R. S. Roskies. "Fourier descriptors for plane closed curves." IEEE Trans. Comput., Vol. C-21 (Mar. 1972), pp. 269-281.

Zucker, S. W., A. Rosenfeld, L. S. Davis. "Picture segmentation by texture discrimination." IEEE Trans. Comput., Vol. C-24, No. 12 (Dec., 1975), pp. 1228-1233.

VITA

Douglas Robert DeVoe

Doctor of Philosophy

Thesis: A FOURIER TRANSFORM TO DETECT PINE SEEDLINGS IN A DIGITAL IMAGE

Major Field: Agricultural Engineering

Biographical:

Education: Graduated from Gaithersburg High School, Gaithersburg, Maryland, in June, 1975; received Bachelor of Science degree in Agricultural Engineering from Oklahoma State University in 1980; received Master of Science degree in Agricultural Engineering from Oklahoma State University in 1982; completed requirements for the Doctor of Philosophy degree at Oklahoma State University in May, 1987.

Professional Experience: Research Engineer, Agricultural Engineering Department, Oklahoma State University, 1983 to present; evening instructor for microcomputer class, Indian Meridian VoTech School, Stillwater, Oklahoma, 1981 to 1983; graduate research assistant, Agricultural Engineering Department, Oklahoma State University, 1980 to 1983; student assistant, Agricultural Engineering Department, Oklahoma State University, 1977 to 1980; student member of the American Society of Agricultural Engineers, Alpha Epsilon, Institute of Electronic and Electrical Engineers; Outstanding Student Acheivement Award, Oklahoma Society of Professional Engineers, May, 1980.